Satellite Navigation Branch, ANG-E66

# ADVANCED RECEIVER AUTONOMOUS INTEGRITY MONITORING PERFORMANCE ANALYSIS REPORT

## February 2023

**Report #10**
**Reporting Period: April 1, 2022 to June 30, 2022**

**FAA William J. Hughes Technical Center**
**Atlantic City International Airport, New Jersey 08405**
**http:/www.nstb.tc.faa.gov**

## DOCUMENT VERSION CONTROL

| VERSION | DESCRIPTION OF CHANGE | DATE |
|---|---|---|
| 0.1 | Initial Draft | 01/11/2023 |
| 0.2 | Tech Edit | 02/10/2023 |
| 0.3 | Peer Review | 02/17/2023 |
| 1.0 | Final Report | 02/17/2023 |

# EXECUTIVE SUMMARY

This is the second quarterly report of 2022 by the United States (U.S.) Federal Aviation Administration (FAA) documenting the performance of the Global Positioning System (GPS) for use in Advanced Receiver Autonomous Integrity Monitoring (ARAIM). ARAIM will be used during aircraft flight operations to assure integrity of the satellite signals, which will permit aircraft to safely navigate worldwide in all phases of flight, including precision landing. The results in this report are intended for further discussion and validation of ARAIM standards. They are not intended for comparison to GPS performance commitments at this time.

This report is produced by the FAA William J. Hughes Technical Center, Satellite Navigation Branch, ANG-E66, in Atlantic City, New Jersey. The Satellite Navigation Branch also provides monitoring and reporting services on U.S. GPS performance and the FAA Wide Area Augmentation System (WAAS) in the "Global Positioning System Standard Positioning Service Performance Analysis Report" and the "Wide Area Augmentation System Performance Analysis Report," respectively. Additionally, the branch monitors performance of the Galileo Global Navigation Satellite System (GNSS) and reports findings in the "Galileo Open Service Performance Analysis Report."

For ARAIM, a global array of GPS receivers is used to monitor signals from every GPS satellite, and those signals are analyzed to determine performance. Standards for ARAIM are evolving, and performance requirements will be published in the near future. In support of those requirements, signal monitoring is required to ensure that performance meets the standards, and to calculate the integrity parameters used to characterize the system. This report provides the current results of that monitoring.

This ARAIM PAN Report #10 includes data and analysis for April 1, 2022 through June 30, 2022. Also presented, for historical comparison and long-term trend analysis, are performance data from January 1, 2008 to June 30, 2022. The report presents measured accuracy and integrity parameters and provides analysis to support the development of the GPS Integrity Support Message (ISM).

The following parameters are currently under consideration for ARAIM user calculation of service integrity: correlation time constant ($t_{correl}$), URA-independent overbound of nominal range bias errors ($b_{nom0}$), URA-dependent overbound of nominal range bias errors ($\gamma_{nom}$), specified probability of a single satellite fault ($R_{sat}$), probability of multiple common cause faults ($P_{const}$) mean fault duration (MFD), service level, and mask. In this report, the parameters $R_{sat}$, $P_{const}$, and MFD are considered the most mature, and they are included. As standards mature, a complete definition of these parameters and their use will be available, and the report will provide the full complement of ARAIM parameters.

In this quarter, GPS continued to perform well, and there were no faults detected. The $R_{sat}$ is currently $10^{-5}$, the $P_{const}$ is currently $10^{-8}$, and the MFD is currently 1 hour. All of these values are consistent with GPS Constellation Service Provider (CSP) commitments.

Individual satellites may be identified using either a space vehicle number (SVN) or a pseudorandom noise (PRN) number. SVN, or sometimes SV, is an unambiguous number that is assigned when the spacecraft is built. PRNs are reused as vehicles are retired or added to the

operational on-orbit constellation. This report uses the term SVN to uniquely identify the individual SV. These terms are the same ones used in Notice Advisory to Navstar Users (NANUs).

The maximum mean, 68%, and 95% values of the aggregated instantaneous Signal-in-Space Range Error (SISRE) across 200 user locations in this quarter were -0.357 m on SVN 73, 1.160 m on SVN 72, and 2.320 m on SVN 72, respectively.

Nominal clock and ephemeris errors for all satellites were described conservatively by the GPS broadcast user range accuracy (URA). In this quarter, URAs overbounded all nominal range errors with the maximum scale factor of 0.822 on SVN 51. The URA value of 2.4 m was broadcast 94.575% of the time, in line with historical performance.

The monthly mean and 95% value of the aggregated instantaneous SISREs in this quarter, of all satellites across 200 user locations, were consistent with historical performance, with all of the means under .500 m and all of the 95% values under 2.500 m. The highest mean was 0.498 m on SVN 73, and the highest 95% value was 2.440 m on SVN 72.

**TABLE OF CONTENTS**

## LIST OF FIGURES

**LIST OF TABLES**

# 1. INTRODUCTION

This report documents the performance of the GNSS, which supports ARAIM for worldwide flight operations. ARAIM uses signals, validated for safety-of-flight use, from multiple satellite constellations without the use of an external augmentation system. ARAIM has the potential to reduce costs for service providers and aircraft operators. In its mature state, it will be able to provide worldwide precision approach capability to any location on earth and support expanded service to remote and unimproved areas.

This report is produced by the U.S. FAA William J. Hughes Technical Center, Satellite Navigation Branch, ANG-E66, in Atlantic City, New Jersey. The Satellite Navigation Branch also provides monitoring and reporting services on U.S. GPS performance and the FAA WAAS. These reports are titled "Global Positioning System Standard Positioning Service Performance Analysis Report" and "Wide Area Augmentation System Performance Analysis Report," respectively. Additionally, the branch monitors performance of the Galileo Global Navigation Satellite System (GNSS) and reports findings in the "Galileo Open Service Performance Analysis Report."

## 1.1 System Overview

ARAIM is intended to support navigation for en route, terminal, and approach flight operations by detecting hazardous faults in the underlying GNSS without the use of external augmentation systems. Making use of the increasing number of available ranging satellites, ARAIM determines the probabilities of one or more simultaneous fault occurrences and calculates an integrity level. ARAIM updates are contained in the ISM, provided by ground monitoring networks that maintain continuous worldwide GNSS coverage. A more detailed operational description is found in the ARAIM Concept of Operation [1].

## 1.2 Purpose

The purpose of this report is to document the ARAIM-related performance parameters of the core constellations that will support ARAIM flight operations and to provide that information to users, operators, and regulators.

## 1.3 Scope

This report currently focuses on the ARAIM-related performance parameters of GPS and the ability to support worldwide flight operations using ARAIM. For future operations, ARAIM is planned to be implemented in phases, first for horizontal navigation, and later expanded to include vertical navigation. As those changes are implemented, these quarterly reports will also be expended to reflect the evolving nature of ARAIM applications.

### 1.4 Report Layout

This report presents several types of ARAIM performance information, including nominal GPS accuracy and statistical distributions, satellite faults and estimated fault rates, historical performance, and verification of some of the underlying assumptions of the defining algorithms.

Data are presented in Section 2.1, including the data source, data cleansing, processing, and analysis. This section also discusses the partitioning of the data and some of the data limitations.

Nominal GPS performance is presented in Section 2.2, including nominal errors and URA, along with statistical error distributions and URA bounding analysis. This section also provides correlation analysis of the nominal error at each user position.

Satellite faults are presented in Section 2.3, including estimated fault rates and historical fault information. Section 2.3 also contains a list with descriptions of any significant or unusual events, such as satellite or monitoring system failures or other unexpected events that impact performance.

## 2. GPS ISM PARAMETER MONITORING

The ARAIM ISM parameter offline -monitoring effort provides for the monitoring of the safety parameters that will be communicated to users through the ISM, including the following:

- An overbound of the probability or rate of single satellite faults ($P_{sat}$ or $R_{sat}$)
- An overbound of the probability or rate of multiple simultaneous faults ($P_{const}$ or $R_{const}$)
- An overbound of nominal range errors (URA)
- A URA-independent overbound of nominal range bias errors ($b_{nom0}$)
- A URA-dependent overbound of nominal range bias errors ($\gamma_{nom}$)
- An overbound of the MFD
- $t_{CORREL}$
- Service Level
- Mask

These parameters are based on CSP commitments and performance history. They must conservatively describe the true satellite behavior in order to be used to predict integrity. Constellation performance is monitored continually to ensure consistency with those commitments.

If required, the results of offline monitoring of the $\gamma_{nom}$, $t_{CORREL}$, $b_{nom0}$, service level, and satellite mask will be included in future reports as standards evolve.

Table 2-1 is a copy of the integrity guarantee as defined in the GPS Standard Positioning Service SPS Performance Standard (PS) [2]. The SPS PS states that the probability of a satellite fault will be no greater than $10^{-5}$ per hour. The commitment further states that users will be notified of major service failures, or the space vehicle (SV) will be removed from service within an average of 1 hour.

**Table 2-1. GPS SPS Instantaneous User Range Error Integrity Standards [2]**

| Signal-in-Space (SIS) Integrity Standard | Conditions and Constraints |
|---|---|
| • Each SPS SIS Component Combination per Table 2.2-2 in the GPS SPS Performance Standard [2]:<br><br>• $\leq 1x10^{-5}$ Probability Over Any Hour of the SPS SIS Instantaneous User Range Error (URE) Exceeding the Not-To-Exceed (NTE) Tolerance Without a Timely Alert | • Applies to any trackable and healthy SPS SIS<br><br>• SPS SIS URE NTE tolerance defined to be 4.42 times the relevant Integrity Assured User Range Accuracy (IAURA) value currently broadcast by the satellite<br><br>• Given that the maximum SPS SIS instantaneous URE did not exceed the NTE tolerance at the start of the hour<br><br>• Unalerted Misleading Signal Information (UMSI) occurs if no timely alert issued after SPS SIS URE NTE tolerance exceeded<br><br>• Worst case for delayed alert is 6 hours<br><br>• Neglecting single-frequency (SF) ionospheric delay model errors |
| **Instantaneous $P_{sat}$ and $P_{const}$** | **Conditions and Constraints** |
| • $\leq 1x10^{-5}$ Fraction of Time When the SPS SIS Instantaneous URE Exceeds the NTE Tolerance Without a Timely Alert ($P_{sat}$)<br><br>• $\leq 1x10^{-8}$ Fraction of Time When the SPS SIS Instantaneous URE from Two or More Satellites Exceeds the NTE Tolerance Due to a Common Cause Without a Timely Alert ($P_{const}$) | • Applies across all trackable and healthy SPS SIS<br><br>• SPS SIS URE NTE tolerance defined to be ±4.42 times the relevant IAURA value currently broadcast by the satellite<br><br>• Average case for delayed alert is 1 hour<br><br>• Neglecting SF ionospheric delay model errors |

## 2.1 Data

### 2.1.1 Data Source and Rate

The offline analysis in this report uses two sources of input data: the GPS broadcast navigation data and post-processed precise data. The broadcast navigation data consists of satellite orbit and clock parameters and includes URA values that indicate the expected level of accuracy. The precise data consists of GPS ephemerides and clock parameters. It is used as the truth reference and has an accuracy of approximately 10 centimeters (cm) [3].

A subset of the GPS broadcast legacy navigation (LNAV) data is available from the International GNSS Service (IGS) in Receiver Independent Exchange (RINEX) navigation file format [4]. Precise GPS ephemerides and clock are available from the National Geospatial-Intelligence Agency (NGA) in the Standard Product #3 (SP3) format [3].

This report includes historical GPS constellation performance from January 1, 2008 to June 30, 2022. Data were analyzed for every 15-minute interval from January 1, 2008 to February 26, 2012 and every 5-minute interval from February 26, 2012 until June 30, 2022. All available data were analyzed during the period. The data intervals are determined by capabilities of the IGS and NGA data sources.

### 2.1.2 Data Collection and Cleansing

A customized tool is used to automate the data downloads on a daily basis. All data are protected by checksums and other basic integrity checks. GPS broadcast navigation data is downloaded from the two IGS archive sites: the Crustal Dynamics Data Information System (CDDIS) [5] and the Scripps Orbit and Permanent Array Center (SOPAC) [6]. Precise data are downloaded from the NGA server [7].

The broadcast navigation data, as received in RINEX format from IGS, sometimes contains defects (such as duplications, inconsistencies, discrepancies, and errors) that can cause false anomalies. A cleansing algorithm is applied to the IGS data to generate "validated" navigation messages, which have as many of these defects removed as possible. This process is based on the algorithm described by Heng [8].

### 2.1.3 Error Computation and Anomaly Detection

For each time step where precise data are available, the most recent prior validated broadcast navigation data are used to propagate the satellite orbits and clocks. To account for clock offset in the precise product, at each epoch, the clock residuals between healthy precise and broadcast products are filtered for outliers; then, a mean correction is applied to the NGA precise clock estimate. At each data point for which both sources indicate a healthy signal and valid data within the fit interval, the satellite position error is determined by calculating the difference between the NGA-derived reference value and the calculated, propagated satellite position, in Earth-Centered, Earth-Fixed (ECEF) coordinates. The errors are segregated into radial, along-track, and cross-track (RAC) errors. The satellite position error is also projected onto Earth at each epoch to produce the maximum projected error (MPE) and projected along the lines of sight to individual user locations on Earth to produce user projected error (UPE). MPE and UPE are two forms of SISRE that are used to evaluate the error distributions.

In this report, 200 evenly distributed user locations around the globe were used to calculate UPE. This density was determined to be sufficient such that a value within 2 cm of the actual MPE will be observed at one or more of the user locations [9]. MPE is computed for each satellite, at each epoch. UPE is computed for each of the 200 user locations, for each satellite in view, for each epoch. A mask angle of 5 degrees is used for MPE and UPE computations. UPEs across satellites are also combined to create a position error at each of the 200 user locations, at each epoch, and a sum of squared residuals statistic is computed. Figure 2-1 shows the 200 MPE user locations.

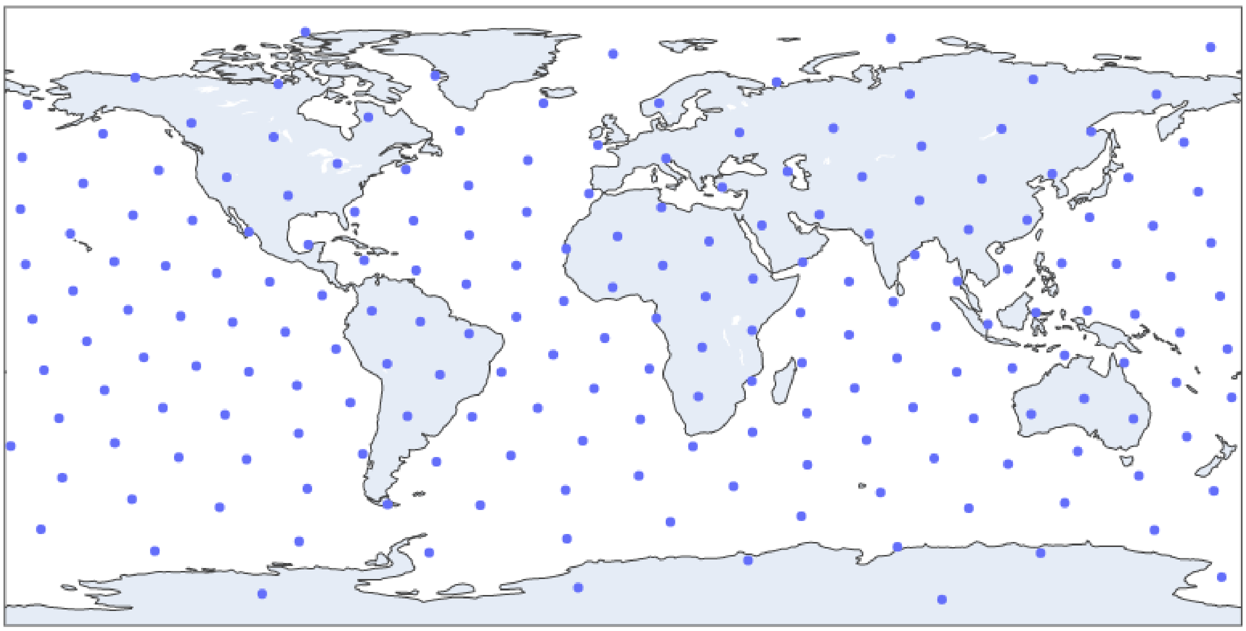

**Figure 2-1. MPE User Locations**

The GPS SPS PS considers an integrity error has occurred if the SISRE is greater than 4.42* URA (see Table 2-1). This report uses a conservative criterion, MPE, to determine if an error has occurred. A potential SIS anomaly is reported when MPE exceeds the 4.42* URA threshold.

Figure 2-2 shows an overview of data availability for the individual months in this quarter. The vertical axis identifies each satellite by their SVN and block type. Each horizontal line indicates health and status for an individual satellite. Green indicates that the vehicle was set healthy, broadcast ephemeris was received, and a valid comparison to the precise ephemeris was obtained. Blue indicates that the vehicle was set unhealthy; therefore, no comparison was available. Purple indicates that no broadcast ephemeris was obtained from the IGS database, and orange indicates that the precise ephemeris was not obtained. In each of those cases, the state of the vehicle was undetermined. The final case, shown by a red circle, indicates that a fault anomaly was detected, and the event will be described in Table 2-11.

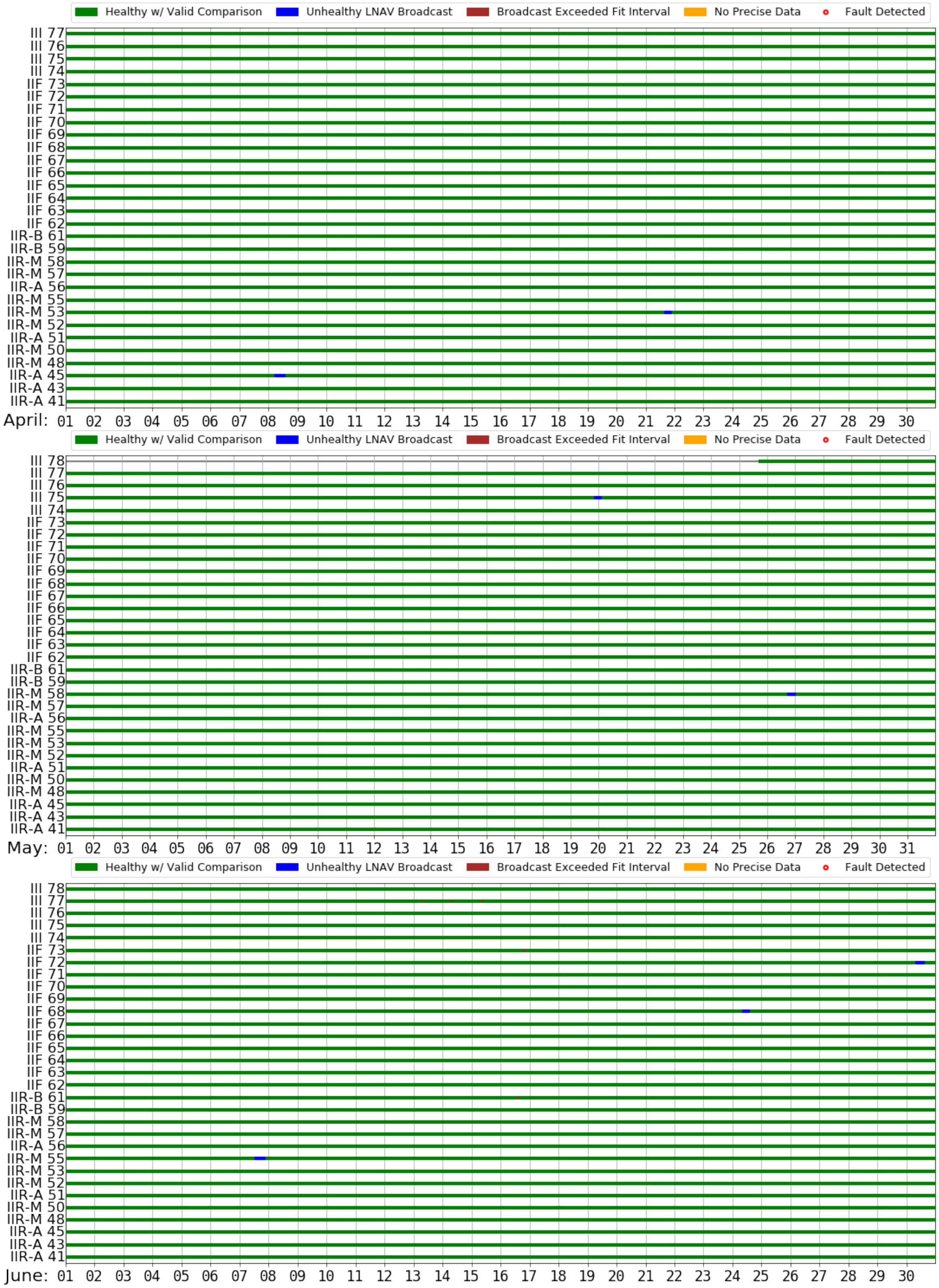


**Figure 2-2. Satellite Data: 2nd Quarter 2022**

Table 2-2 shows the sample counts and the percentages of satellite data for this quarter. A total of 769,537 samples were evaluated this quarter with no fault detected. The data that were not evaluated corresponded to satellites flagged "Unhealthy." During the quarter, several satellites were set to "Unusable" for short periods of time. These include SVN 45 (PRN21) on April 8 (see NANU2022019); SVN 53 (PRN17) on April 21 (see NANU2022021); SVN 75 (PRN18) on May 19 (see NANU2022023); SVN 58 (PRN12) on May 26 (see NANU2022026); SVN 68 (PRN09) on June 24 (see NANU2021030); and SVN 72 (PRN08) on June 30 (see NANU2021032). In addition, SVN 78 (PRN11) became usable on May 25 (see NANU2022025).

**Table 2-2. Satellite Data: 2nd Quarter 2022**

| Data Evaluation | Number of Samples | Percentage of Total |
|---|---|---|
| Valid Data Evaluation | 796125 | 99.929% |
| No Evaluation due to SV Unhealthy | 538 | 0.068% |
| No Evaluation due to Exceeding 4-hour Fit Interval | 12 | 0.002% |
| No Evaluation due to Precise Data Event Flag | 14 | 0.002% |
| No Evaluation due to Broadcast Data Unavailable | 0 | 0.000% |
| No Evaluation due to Precise Data Unavailable | 0 | 0.000% |
| Faults | 0 | 0.000% |

### 2.1.4 Data Partitioning

Performance is analyzed and presented using several data partitions to show various dependencies. These include time, the individual satellite, the satellite block type, the URA value, or combinations of these. See Table 2-3 for this quarter's current PRN assignments, which are used in this report.

**Table 2-3. PRN Assignment by SVN**

| PRN | SVN | Block Type |
|---|---|---|
| 1 | 63 | IIF |
| 2 | 61 | IIR |
| 3 | 69 | IIF |
| 4 | 74 | III |
| 5 | 50 | IIR-M |
| 6 | 67 | IIF |
| 7 | 48 | IIR-M |
| 8 | 72 | IIF |
| 9 | 68 | IIF |
| 10 | 73 | IIF |
| 11 | 78 | III |
| 12 | 58 | IIR-M |
| 13 | 43 | IIR |
| 14 | 77 | III |
| 15 | 55 | IIR-M |
| 16 | 56 | IIR |
| 17 | 53 | IIR-M |
| 18 | 75 | III |
| 19 | 59 | IIR |
| 20 | 51 | IIR |
| 21 | 45 | IIR |
| 22 | 41 | IIR |
| 23 | 76 | III |
| 24 | 65 | IIF |
| 25 | 62 | IIF |
| 26 | 71 | IIF |
| 27 | 66 | IIF |
| 28 | - | - |
| 29 | 57 | IIR-M |
| 30 | 64 | IIF |
| 31 | 52 | IIR-M |
| 32 | 70 | IIF |

### 2.1.5 Data Limitations

SIS anomalies are listed in Table 2-11. There are some limitations of SIS anomaly reporting due to potential errors in the source data or missing source data. Some limitations include:

- False SIS anomalies may be reported due to errors in the precise ephemerides/clock or errors in the validated navigation messages.
- Short-duration SIS anomalies may not be reported if they happen to fall within the 5- or 15-minute gaps of the precise ephemerides/clocks.
- True SIS anomalies may not be detected if the precise ephemerides/clocks, or LNAV data, are temporarily missing or incorrect, for any reason.

### 2.1.6 Data Analysis

The goal of the data analysis process is to determine whether the behavior of the observed data is consistent with the underlying assumptions and the CSP commitments.

The first step in the process is to remove, as completely as possible, any errors that have been introduced by the data collection process itself. These include transmission errors, incomplete data sets from an individual source, conflicting data from separate sources, or any other known error type.

The next step is the nominal performance analysis, to ensure that the nominal observed error distributions are Gaussian and bounded by the URA, as defined in the SPS PS. The error characteristic is observed in the probability density function (PDF) plots of the RAC, clock, and SISRE errors.

A sigma overbounding and the ratio of the minimum overbounding sigma to the broadcast URA and the Gaussian curve are computed. A PDF of SISREs is used to observe the core of the error distribution, and a cumulative distribution function (CDF) is used to observe the tail behavior.

Correlation of errors is also checked to ensure that the individual ranging errors do not combine to form unexpectedly large position errors. The sum of the squares of the URA-normalized residuals is computed for each time step and user, and all samples are combined in a single distribution. Correlated residuals will be indicated by a sum of square residuals distribution that exceeds a chi-square distribution.

After the signal performance analysis, any potential faults are analyzed. That analysis will provide, at a minimum, the date, time, and duration of the fault, as well as the overall effect on fault rates and probabilities. A description of the potential fault will be provided, as well as the basis used to identify it. If possible, the initial cause of the fault will also be determined and described, along with any associated maintenance action taken.

The data in this report are presented using different views and data partitions to describe performance more completely. The different types of views include statistical plots, such as probability, residual error over time, histograms, one minus CDF (1-CDF) plots, and data tables, partitioned by satellite, block types, and composite. These views show: overbounding of the measured data by the integrity parameters, comparison of residuals (based on an independent reference) of orbital and clock parameters, presentation of range error in different units and coordinate systems, projected user errors, and comparison to historical performance.

## 2.2 Nominal Accuracy and URA Bounding

GPS satellites broadcast URA values to indicate the expected level of accuracy. The URA represents a 1-sigma value that conservatively characterizes the nominal signal accuracy. Offline monitoring of the URA parameter assesses the integrity of the ephemeris and clock data in the broadcast navigation messages, by evaluating the URA bounding performance of nominal, fault-free range errors. The observed error distributions are examined to evaluate how well the URA describes them.

### 2.2.1 Broadcast URA

Broadcast URA values are shown in Figure 2-3 and Table 2-4 for data from January 1, 2008 to June 30, 2022, and Figure 2-4 and Table 2-5 for the 2nd quarter 2022. The figures and tables show the relative frequency of different broadcast values by satellite, block type, and across the whole constellation.

The URA index of 1, corresponding to 2.4 m, is the most common URA value since January 1, 2008. This value was sent 93.744% of the time for all satellites, and the next most common index value of 2, corresponding to 3.4 m, was sent 5.939% of the time; both values combined accounted for 99.683% of all broadcast URA.

For this quarter, the URA value of 2.4 m is sent 94.575% of the time and 3.4 m is sent is 5.088% of the time; both values combined accounted for 99.663% of all broadcast URA.

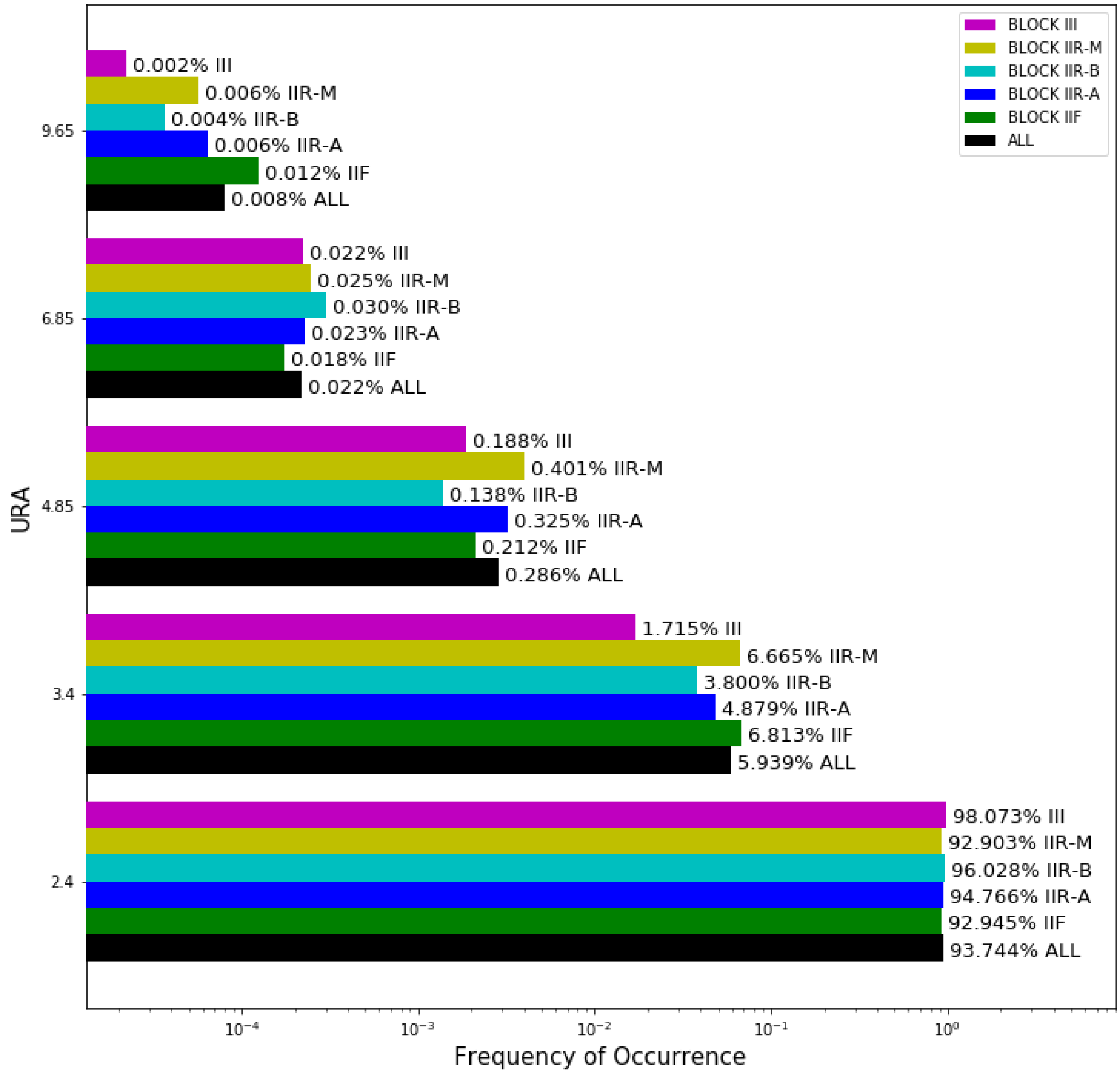


**Figure 2-3. Relative Frequency of URA: January 1, 2008 to June 30, 2022**

**Table 2-4. Relative Frequency of URA: January 1, 2008 to June 30, 2022**

| Block/SVN | Relative Frequency (%) of Broadcast URA Values | | | | |
|---|---|---|---|---|---|
| | 2.4 m | 3.4 m | 4.85 m | 6.85 m | 9.65 m |
| ALL | 93.744 | 5.939 | 0.286 | 0.022 | 0.008 |
| BLOCK IIF | 92.945 | 6.813 | 0.212 | 0.018 | 0.012 |
| BLOCK IIR-A | 94.766 | 4.879 | 0.325 | 0.023 | 0.006 |
| BLOCK IIR-B | 96.028 | 3.800 | 0.138 | 0.030 | 0.004 |
| BLOCK IIR-M | 92.903 | 6.665 | 0.401 | 0.025 | 0.006 |
| BLOCK III | 98.073 | 1.715 | 0.188 | 0.022 | 0.002 |
| 41 | 92.528 | 7.185 | 0.241 | 0.030 | 0.015 |
| 43 | 95.104 | 4.826 | 0.052 | 0.010 | 0.008 |
| 45 | 92.528 | 6.237 | 1.199 | 0.037 | 0.000 |
| 48 | 93.248 | 5.459 | 1.217 | 0.073 | 0.003 |
| 50 | 98.023 | 1.898 | 0.060 | 0.010 | 0.007 |
| 51 | 97.188 | 2.715 | 0.078 | 0.013 | 0.006 |
| 52 | 94.072 | 5.548 | 0.342 | 0.027 | 0.012 |
| 53 | 83.844 | 15.091 | 1.039 | 0.012 | 0.010 |
| 55 | 96.620 | 3.330 | 0.034 | 0.016 | N/A |
| 56 | 96.188 | 3.737 | 0.046 | 0.024 | 0.005 |
| 57 | 88.627 | 11.276 | 0.078 | 0.011 | 0.008 |
| 58 | 96.128 | 3.818 | 0.030 | 0.023 | N/A |
| 59 | 96.879 | 3.057 | 0.029 | 0.030 | 0.005 |
| 61 | 95.176 | 4.543 | 0.248 | 0.030 | 0.002 |
| 62 | 95.959 | 3.957 | 0.072 | 0.008 | 0.004 |
| 63 | 94.396 | 5.445 | 0.140 | 0.009 | 0.010 |
| 64 | 94.981 | 4.942 | 0.058 | 0.019 | N/A |
| 65 | 75.607 | 23.906 | 0.468 | 0.017 | 0.001 |
| 66 | 95.075 | 4.779 | 0.141 | 0.006 | N/A |
| 67 | 97.610 | 2.292 | 0.051 | 0.028 | 0.020 |
| 68 | 96.931 | 2.987 | 0.052 | 0.016 | 0.014 |
| 69 | 90.138 | 8.537 | 1.243 | 0.047 | 0.035 |
| 70 | 96.244 | 3.597 | 0.081 | 0.031 | 0.047 |
| 71 | 95.052 | 4.860 | 0.041 | 0.019 | 0.027 |
| 72 | 87.637 | 12.142 | 0.193 | 0.022 | 0.007 |
| 73 | 98.446 | 1.547 | 0.007 | N/A | N/A |
| 74 | 99.302 | 0.624 | 0.051 | 0.019 | 0.005 |
| 75 | 97.990 | 1.855 | 0.091 | 0.061 | 0.003 |
| 76 | 97.779 | 1.905 | 0.315 | N/A | N/A |
| 77 | 96.745 | 2.845 | 0.410 | N/A | N/A |
| 78 | 95.684 | 4.316 | N/A | N/A | N/A |

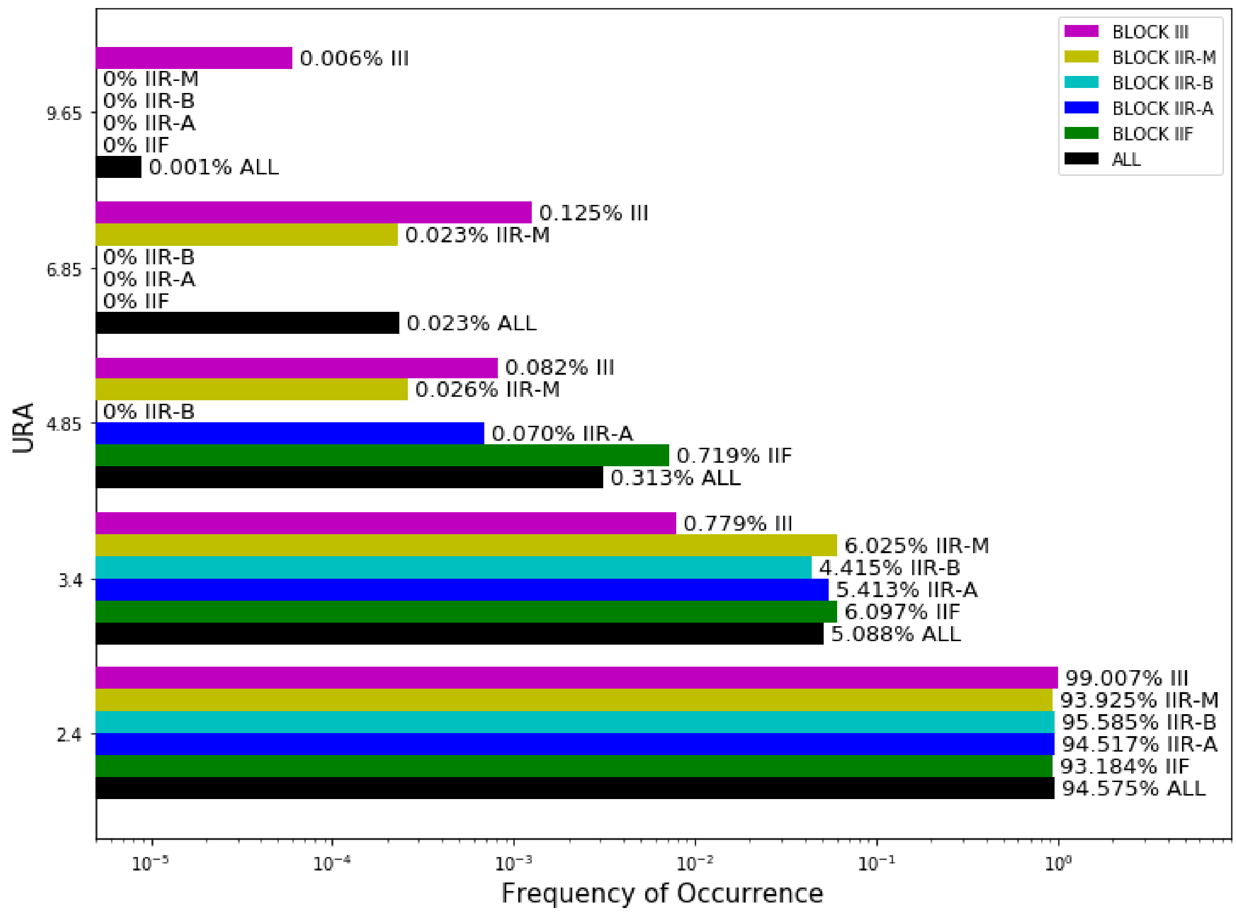


**Figure 2-4. Relative Frequency of URA: 2nd Quarter 2022**

**Table 2-5. Relative Frequency of URA: 2nd Quarter 2022**

| Block/SVN | Relative Frequency (%) of Broadcast URA Values | | | | |
|---|---|---|---|---|---|
| | 2.4 m | 3.4 m | 4.85 m | 6.85 m | 9.65 m |
| ALL | 94.575 | 5.088 | 0.313 | 0.023 | 0.001 |
| BLOCK IIF | 93.184 | 6.097 | 0.719 | N/A | N/A |
| BLOCK IIR-A | 94.517 | 5.413 | 0.070 | N/A | N/A |
| BLOCK IIR-B | 95.585 | 4.415 | N/A | N/A | N/A |
| BLOCK IIR-M | 93.925 | 6.025 | 0.026 | 0.023 | N/A |
| BLOCK III | 99.007 | 0.779 | 0.082 | 0.125 | 0.006 |
| 41 | 89.873 | 10.127 | N/A | N/A | N/A |
| 43 | 99.641 | 0.359 | N/A | N/A | N/A |
| 45 | 87.394 | 12.269 | 0.337 | N/A | N/A |
| 48 | 99.302 | 0.698 | N/A | N/A | N/A |
| 50 | 99.435 | 0.565 | N/A | N/A | N/A |
| 51 | 98.855 | 1.133 | 0.011 | N/A | N/A |
| 52 | 91.701 | 8.299 | N/A | N/A | N/A |
| 53 | 82.814 | 16.841 | 0.184 | 0.161 | N/A |
| 55 | 99.422 | 0.578 | N/A | N/A | N/A |
| 56 | 96.795 | 3.205 | N/A | N/A | N/A |
| 57 | 87.767 | 12.233 | N/A | N/A | N/A |
| 58 | 97.038 | 2.962 | N/A | N/A | N/A |
| 59 | 94.521 | 5.479 | N/A | N/A | N/A |
| 61 | 96.649 | 3.351 | N/A | N/A | N/A |
| 62 | 96.360 | 3.640 | N/A | N/A | N/A |
| 63 | 98.115 | 1.885 | N/A | N/A | N/A |
| 64 | 97.016 | 2.984 | N/A | N/A | N/A |
| 65 | 97.775 | 2.225 | N/A | N/A | N/A |
| 66 | 84.470 | 15.530 | N/A | N/A | N/A |
| 67 | 97.081 | 2.862 | 0.057 | N/A | N/A |
| 68 | 99.442 | 0.371 | 0.187 | N/A | N/A |
| 69 | 71.486 | 20.131 | 8.383 | N/A | N/A |
| 70 | 98.844 | 1.156 | N/A | N/A | N/A |
| 71 | 97.600 | 2.400 | N/A | N/A | N/A |
| 72 | 82.829 | 17.171 | N/A | N/A | N/A |
| 73 | 97.172 | 2.828 | N/A | N/A | N/A |
| 74 | 99.222 | 0.778 | N/A | N/A | N/A |
| 75 | 98.807 | 0.252 | 0.363 | 0.551 | 0.027 |
| 76 | 99.496 | 0.504 | N/A | N/A | N/A |
| 77 | 99.828 | 0.172 | N/A | N/A | N/A |
| 78 | 95.684 | 4.316 | N/A | N/A | N/A |

### 2.2.2 Nominal Accuracy

Orbit, clock, and projected range errors are shown in this section for the current quarter. The errors consist of RAC, clock, and the aggregated SISREs across 200 user locations, for the quarter. Table 2-6 shows the mean, 68%, and 95% values for RAC, clock, and SISRE errors by satellite, block type, and the aggregated total. The maximum SISRE mean was -0.257 m on SVN 63, the maximum SISRE 68% value was 1.160 m on SVN 72, and the maximum SISRE 95% was 2.320 m on SVN 72.

Figure 2-5 shows plots of the same values by satellite and in composite. The green segment represents the (68%) area of the error distribution, and the upper and lower fences represent the (95%) area of the error distribution. The center tick value is the mean of the nominal error distribution. (Satellite range errors exceeding 4.42 times URA are excluded from this nominal assessment.) The scale for each parameter is adjusted to focus on the range of most interest.

Figure 2-6 shows the aggregated PDF of the same errors. For this quarter, the majority of the errors appear nearly Gaussian, with the radial errors as the smallest and along-track errors as the largest. The aggregated SISRE across 200 user locations and clock errors agree fairly well. There are significantly larger errors below the $10^{-5}$ level. These are consistent with the SPS PS, which guarantees performance to the $10^{-5}$ level.

**Table 2-6. RAC, Clock, and SISRE Errors: 2nd Quarter 2022**

| SVN | Block | Radial | | | Along-Track | | | Cross-Track | | | Clock | | | SISRE | | |
|---|---|---|---|---|---|---|---|---|---|---|---|---|---|---|---|---|
| | | Mean | 68% | 95% | Mean | 68% | 95% | Mean | 68% | 95% | Mean | 68% | 95% | Mean | 68% | 95% |
| 41 | BLOCK IIR-A | 0.044 | 0.120 | 0.280 | -0.477 | 0.880 | 2.080 | 0.036 | 0.600 | 1.280 | -0.107 | 0.280 | 0.640 | 0.150 | 0.340 | 0.760 |
| 43 | | 0.010 | 0.160 | 0.240 | -0.092 | 0.760 | 1.600 | -0.035 | 0.480 | 1.040 | 0.011 | 0.440 | 1.040 | -0.002 | 0.420 | 1.020 |
| 45 | | -0.017 | 0.160 | 0.320 | 0.111 | 1.000 | 2.120 | 0.000 | 0.560 | 1.120 | 0.022 | 0.280 | 0.560 | -0.039 | 0.340 | 0.680 |
| 51 | | -0.010 | 0.120 | 0.240 | 0.375 | 0.800 | 1.800 | -0.024 | 0.600 | 1.120 | 0.053 | 0.280 | 0.640 | -0.063 | 0.320 | 0.740 |
| 56 | | -0.012 | 0.160 | 0.280 | 0.099 | 0.960 | 2.000 | 0.003 | 0.520 | 0.960 | -0.027 | 0.240 | 0.480 | 0.015 | 0.260 | 0.540 |
| 59 | BLOCK IIR-B | 0.036 | 0.160 | 0.280 | -0.230 | 0.760 | 1.600 | 0.034 | 0.480 | 1.040 | 0.017 | 0.200 | 0.440 | 0.018 | 0.260 | 0.520 |
| 61 | | -0.059 | 0.160 | 0.320 | 1.058 | 1.480 | 3.160 | -0.039 | 0.600 | 1.360 | -0.069 | 0.280 | 0.520 | 0.011 | 0.340 | 0.720 |
| 48 | BLOCK IIR-M | 0.010 | 0.160 | 0.280 | -0.035 | 0.840 | 2.000 | 0.025 | 0.560 | 1.120 | -0.003 | 0.480 | 1.080 | 0.013 | 0.480 | 1.160 |
| 50 | | 0.028 | 0.200 | 0.320 | -0.281 | 0.880 | 1.680 | 0.048 | 0.520 | 1.000 | -0.061 | 0.280 | 0.520 | 0.088 | 0.280 | 0.560 |
| 52 | | 0.018 | 0.120 | 0.240 | -0.191 | 0.680 | 1.320 | -0.023 | 0.440 | 0.800 | -0.253 | 0.440 | 0.880 | 0.270 | 0.460 | 0.940 |
| 53 | | 0.012 | 0.200 | 0.360 | 0.087 | 1.440 | 3.080 | 0.040 | 0.840 | 1.520 | -0.029 | 0.560 | 1.640 | 0.041 | 0.600 | 1.680 |
| 55 | | -0.010 | 0.120 | 0.200 | 0.306 | 0.760 | 1.520 | -0.029 | 0.480 | 0.880 | -0.082 | 0.240 | 0.400 | 0.072 | 0.220 | 0.460 |
| 57 | | 0.009 | 0.200 | 0.320 | 0.352 | 0.760 | 1.560 | 0.093 | 0.440 | 0.840 | -0.025 | 0.320 | 1.040 | 0.033 | 0.360 | 1.080 |
| 58 | | 0.008 | 0.200 | 0.320 | 0.008 | 1.000 | 2.240 | 0.035 | 0.560 | 1.160 | -0.071 | 0.240 | 0.480 | 0.079 | 0.280 | 0.580 |
| 62 | BLOCK IIF | -0.018 | 0.240 | 0.440 | 0.396 | 1.040 | 2.240 | 0.057 | 0.520 | 1.120 | -0.059 | 0.280 | 0.520 | 0.041 | 0.400 | 0.720 |
| 63 | | 0.004 | 0.200 | 0.360 | -0.152 | 0.680 | 1.560 | -0.006 | 0.440 | 0.880 | 0.061 | 0.200 | 0.400 | -0.058 | 0.280 | 0.560 |
| 64 | | -0.001 | 0.200 | 0.360 | 0.000 | 0.640 | 1.400 | 0.083 | 0.480 | 0.880 | 0.262 | 0.400 | 0.680 | -0.263 | 0.420 | 0.820 |
| 65 | | -0.056 | 0.200 | 0.360 | 0.876 | 1.280 | 2.360 | 0.027 | 0.560 | 1.080 | 0.054 | 0.240 | 0.440 | -0.108 | 0.360 | 0.700 |
| 66 | | -0.023 | 0.160 | 0.280 | 0.193 | 0.760 | 1.760 | 0.034 | 0.400 | 0.880 | -0.116 | 0.240 | 0.480 | 0.094 | 0.300 | 0.600 |
| 67 | | 0.039 | 0.200 | 0.360 | -0.627 | 1.080 | 2.400 | 0.018 | 0.480 | 0.960 | 0.024 | 0.240 | 0.440 | 0.014 | 0.320 | 0.640 |
| 68 | | 0.022 | 0.160 | 0.280 | -0.096 | 0.720 | 1.640 | 0.037 | 0.400 | 0.840 | -0.010 | 0.200 | 0.320 | 0.032 | 0.220 | 0.480 |
| 69 | | -0.049 | 0.160 | 0.320 | 0.953 | 1.480 | 2.880 | 0.044 | 0.840 | 1.560 | 0.133 | 0.600 | 1.560 | -0.181 | 0.640 | 1.600 |
| 70 | | 0.029 | 0.160 | 0.280 | -0.360 | 0.840 | 1.720 | -0.043 | 0.520 | 0.960 | -0.067 | 0.200 | 0.360 | 0.097 | 0.260 | 0.500 |
| 71 | | 0.002 | 0.200 | 0.360 | 0.089 | 0.800 | 1.600 | 0.053 | 0.520 | 0.920 | -0.028 | 0.240 | 0.480 | 0.030 | 0.300 | 0.620 |
| 72 | | 0.028 | 0.200 | 0.400 | -0.399 | 1.040 | 2.080 | 0.004 | 0.640 | 1.160 | 0.190 | 1.160 | 2.280 | -0.162 | 1.160 | 2.320 |
| 73 | | 0.009 | 0.200 | 0.320 | -0.037 | 0.920 | 2.080 | -0.011 | 0.840 | 1.480 | 0.366 | 0.600 | 1.000 | -0.357 | 0.600 | 1.060 |
| 74 | BLOCK III | 0.027 | 0.120 | 0.240 | -0.214 | 0.720 | 1.480 | -0.014 | 0.480 | 0.880 | 0.006 | 0.160 | 0.360 | 0.021 | 0.220 | 0.440 |
| 75 | | -0.058 | 0.160 | 0.320 | 0.570 | 0.840 | 1.920 | -0.051 | 0.640 | 1.200 | -0.019 | 0.200 | 0.400 | -0.038 | 0.280 | 0.580 |
| 76 | | -0.071 | 0.160 | 0.280 | 1.297 | 1.920 | 3.320 | 0.068 | 0.560 | 1.240 | -0.124 | 0.240 | 0.400 | 0.053 | 0.320 | 0.680 |
| 77 | | -0.013 | 0.160 | 0.280 | 0.194 | 0.800 | 2.040 | 0.018 | 0.520 | 1.000 | -0.020 | 0.200 | 0.400 | 0.007 | 0.260 | 0.520 |
| 78 | | -0.015 | 0.120 | 0.240 | 0.226 | 0.720 | 1.360 | 0.032 | 0.520 | 0.920 | -0.065 | 0.200 | 0.400 | 0.050 | 0.240 | 0.500 |

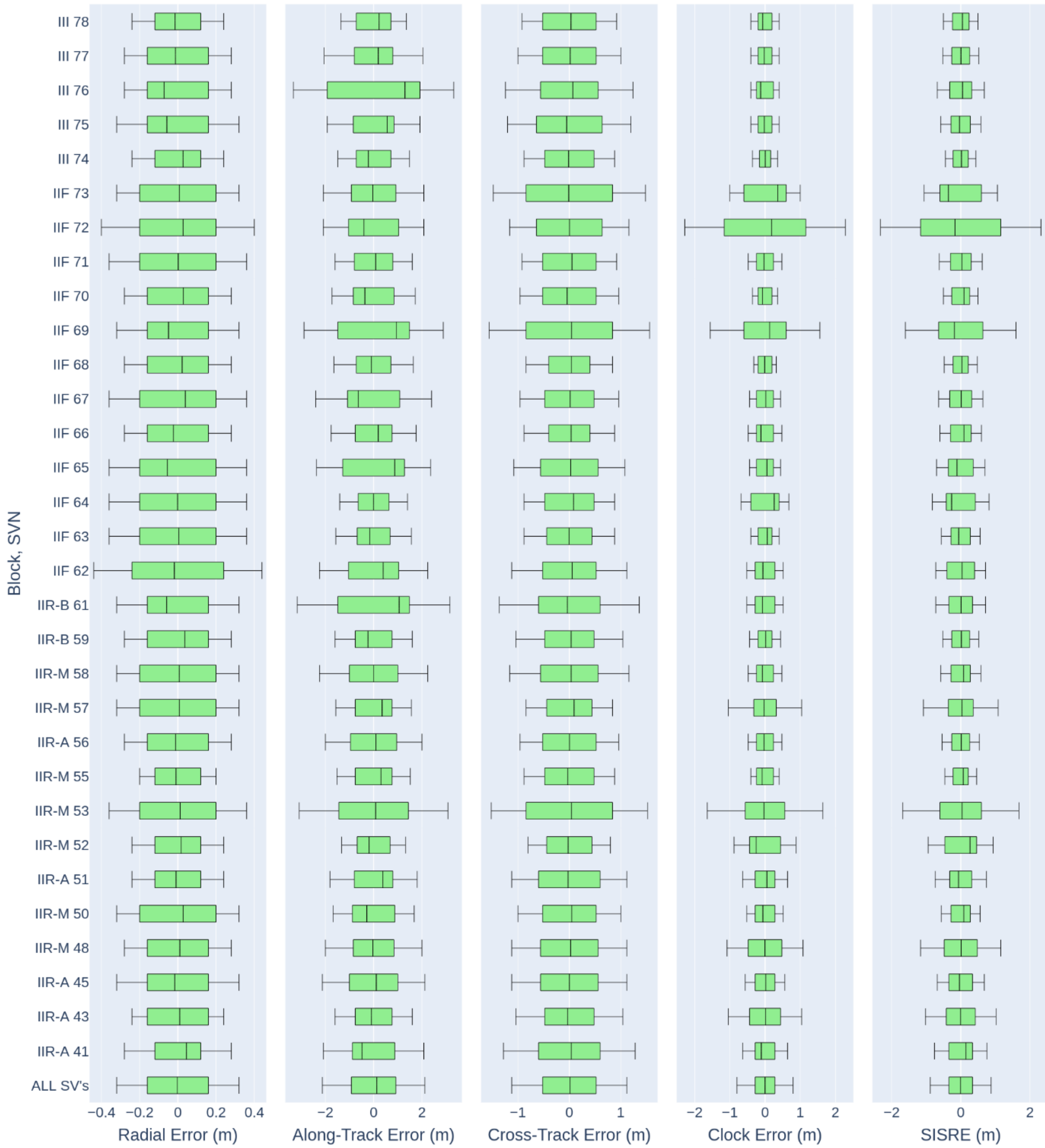


**Figure 2-5. RAC, Clock, and SISRE Errors Box Plot: 2nd Quarter 2022**

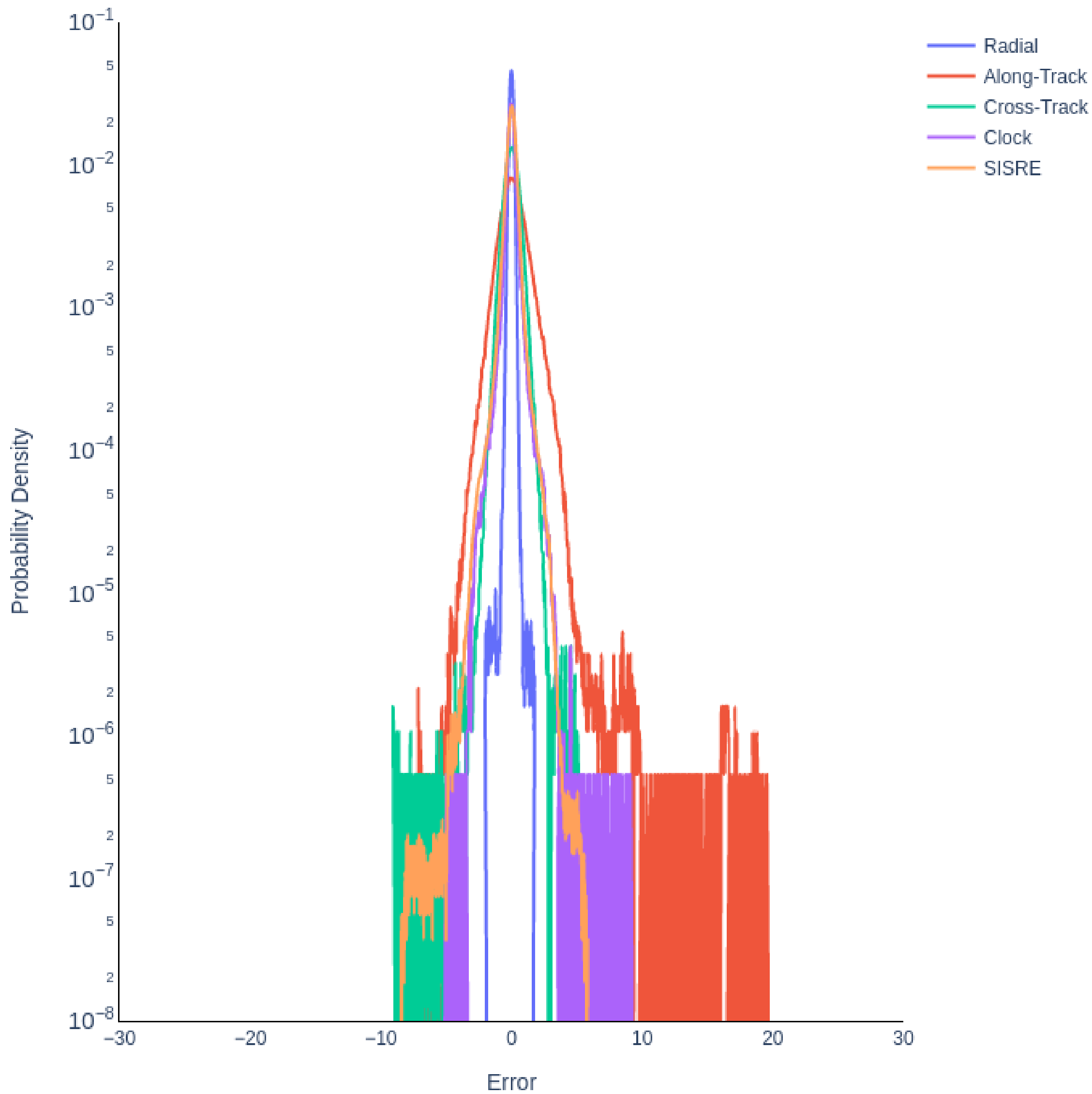


**Figure 2-6. RAC, Clock, and SISRE Errors (PDF): 2nd Quarter 2022**

Historical performance data are presented by satellite for all available data since January 1, 2008. Monthly mean SISRE errors are shown in Figure 2-7 through Figure 2-10, and the monthly 95% error bounds are shown in Figure 2-11 to Figure 2-14. Table 2-7 shows the absolute value of the minimum and maximum of the monthly means and 95% values for all available data. The monthly means were all under 0.95 m with the high value of 0.904 m on SVN 63; and the monthly 95% values were all under 2.8 m with the high value of 2.780 m on SVN 48.


.

**Figure 2-7. Monthly Mean SISRE for SVN 41–SVN 53: January 1, 2008 to June 30, 2022**


**Figure 2-8. Monthly Mean SISRE for SVN 55–SVN 63: January 1, 2008 to June 30, 2022**

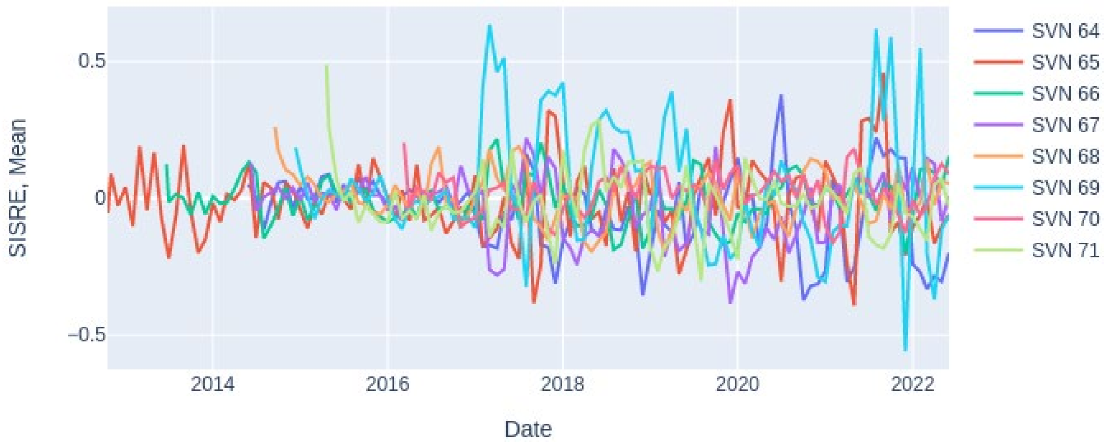


**Figure 2-9. Monthly Mean SISRE for SVN 64–SVN 71: January 1, 2008 to June 30, 2022**

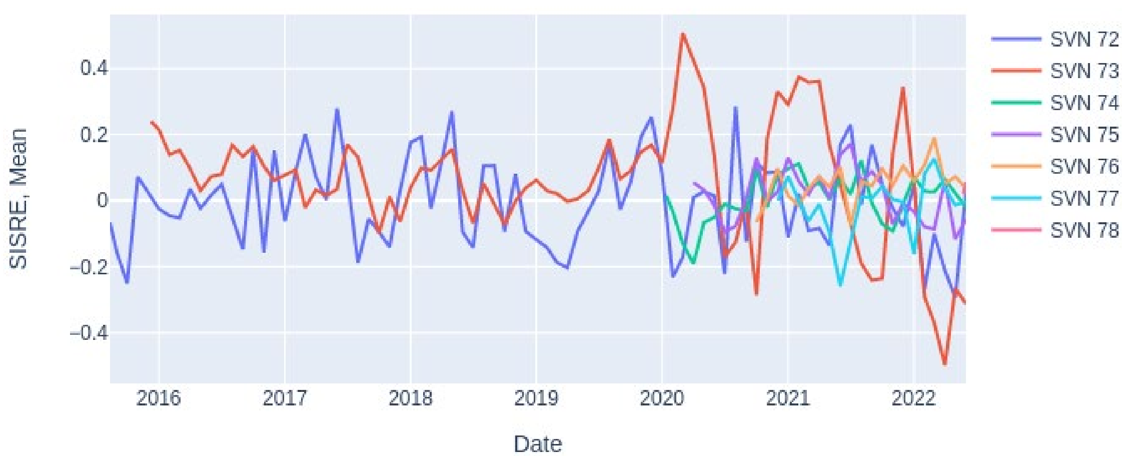


**Figure 2-10. Monthly Mean SISRE for SVN 72–SVN 78: January 1, 2008 to June 30, 2022**

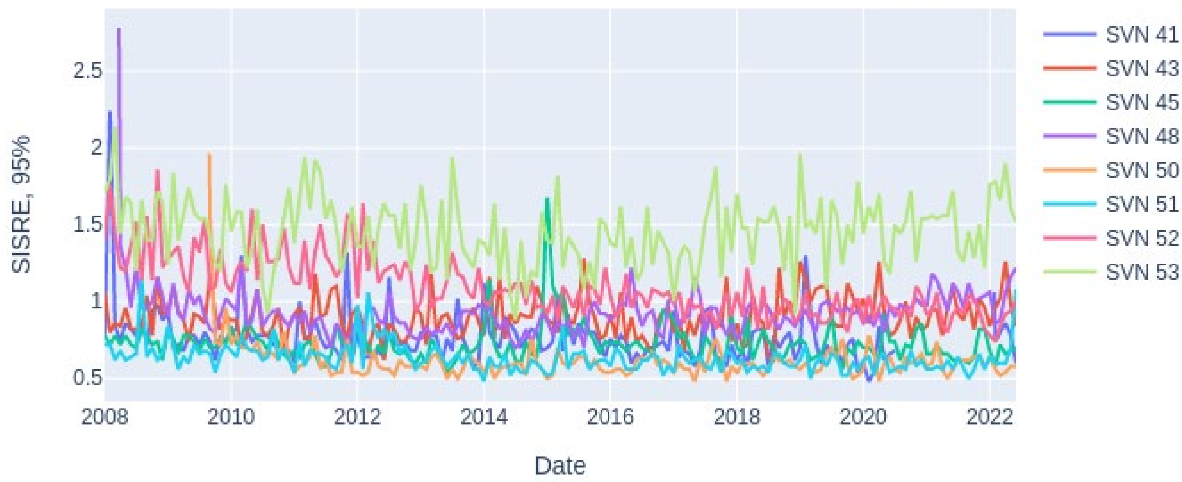


**Figure 2-11. Monthly 95% SISRE for SVN 41–SVN 53: January 1, 2008 to June 30, 2022**

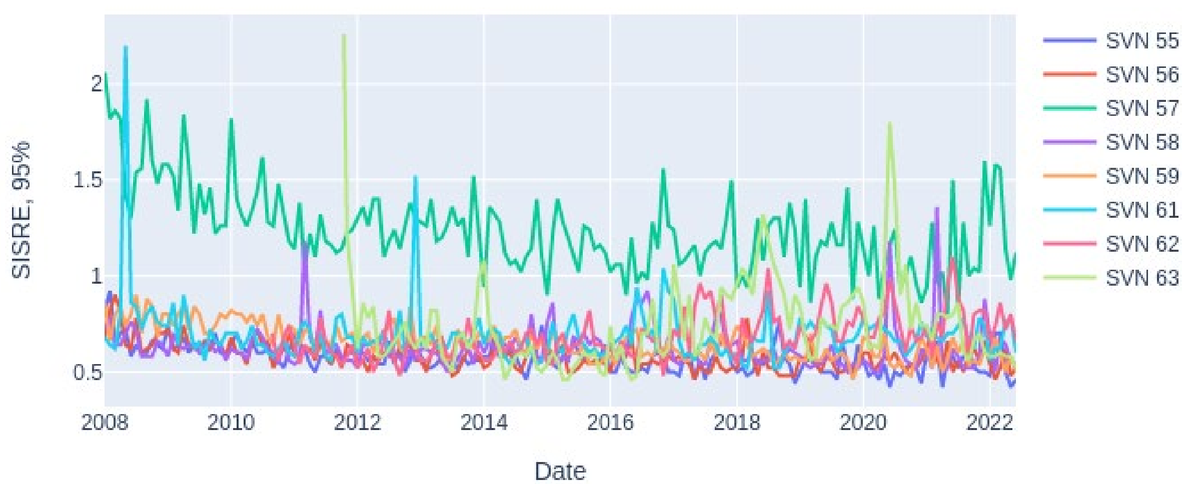


**Figure 2-12. Monthly 95% SISRE for SVN 55–SVN 63: January 1, 2008 to June 30, 2022**


**Figure 2-13. Monthly 95% SISRE for SVN 64–SVN 71: January 1, 2008 to June 30, 2022**


**Figure 2-14. Monthly 95% SISRE for SVN 72–SVN 78: January 1, 2008 to June 30, 2022**

**Table 2-7. Monthly Mean and 95% SISRE: January 1, 2008 to June 30, 2022**

| SVN | Mean (m) | | 95% (m) | |
|---|---|---|---|---|
| | Max | Min | Max | Min |
| 41 | 0.329 | 0.000 | 2.240 | 0.480 |
| 43 | 0.242 | 0.000 | 1.280 | 0.620 |
| 45 | 0.182 | 0.000 | 1.680 | 0.540 |
| 48 | 0.821 | 0.000 | 2.780 | 0.700 |
| 50 | 0.153 | 0.000 | 1.960 | 0.480 |
| 51 | 0.218 | 0.000 | 1.160 | 0.480 |
| 52 | 0.301 | 0.000 | 1.860 | 0.740 |
| 53 | 0.410 | 0.001 | 2.140 | 0.880 |
| 55 | 0.195 | 0.000 | 0.920 | 0.420 |
| 56 | 0.265 | 0.000 | 0.900 | 0.460 |
| 57 | 0.320 | 0.000 | 2.060 | 0.800 |
| 58 | 0.254 | 0.000 | 1.360 | 0.500 |
| 59 | 0.244 | 0.000 | 0.900 | 0.460 |
| 61 | 0.629 | 0.002 | 2.200 | 0.520 |
| 62 | 0.381 | 0.000 | 1.100 | 0.480 |
| 63 | 0.904 | 0.001 | 2.260 | 0.460 |
| 64 | 0.379 | 0.001 | 2.100 | 0.400 |
| 65 | 0.459 | 0.004 | 2.680 | 0.560 |
| 66 | 0.217 | 0.001 | 1.180 | 0.460 |
| 67 | 0.383 | 0.000 | 1.160 | 0.400 |
| 68 | 0.261 | 0.000 | 1.260 | 0.420 |
| 69 | 0.633 | 0.001 | 1.900 | 0.440 |
| 70 | 0.203 | 0.001 | 1.680 | 0.400 |
| 71 | 0.488 | 0.002 | 1.880 | 0.440 |
| 72 | 0.293 | 0.002 | 2.500 | 1.580 |
| 73 | 0.508 | 0.002 | 1.460 | 0.460 |
| 74 | 0.191 | 0.003 | 0.600 | 0.380 |
| 75 | 0.171 | 0.003 | 0.680 | 0.420 |
| 76 | 0.191 | 0.004 | 0.780 | 0.400 |
| 77 | 0.259 | 0.000 | 0.880 | 0.460 |
| 78 | 0.056 | 0.019 | 0.600 | 0.480 |

Monthly mean and 95% SISREs for each satellite for this quarter are shown in Figure 2-15 to Figure 2-22, and the minimum and maximum values are shown in Table 2-8. All of the means were under .500 m, with the high values of 0.498 m on SVN 73. All of the 95% values were below 2.5 m with the high value of 2.440 m on SVN 72.

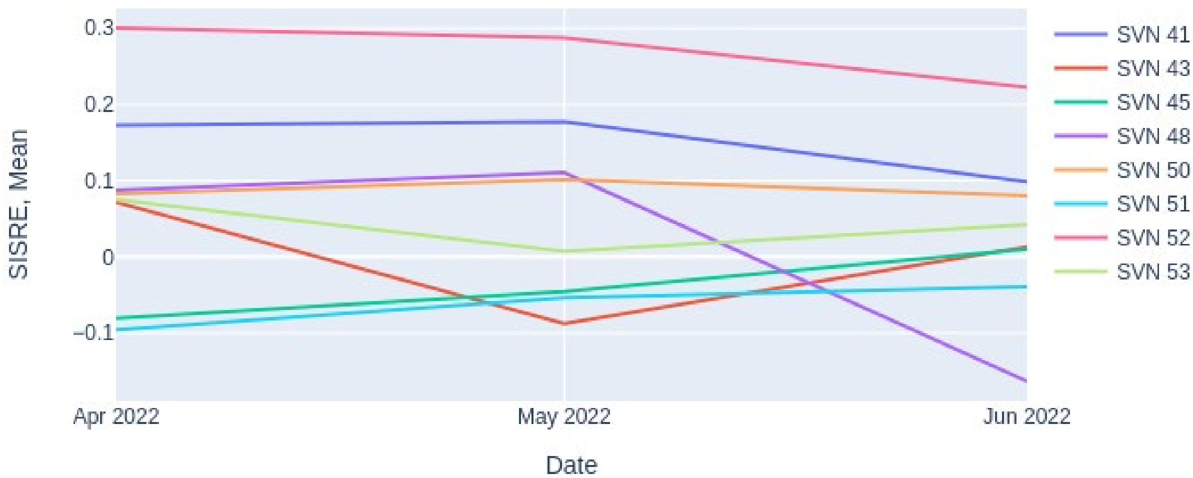


**Figure 2-15. Monthly Mean SISRE for SVN 41–SVN 53: 2nd Quarter 2022**

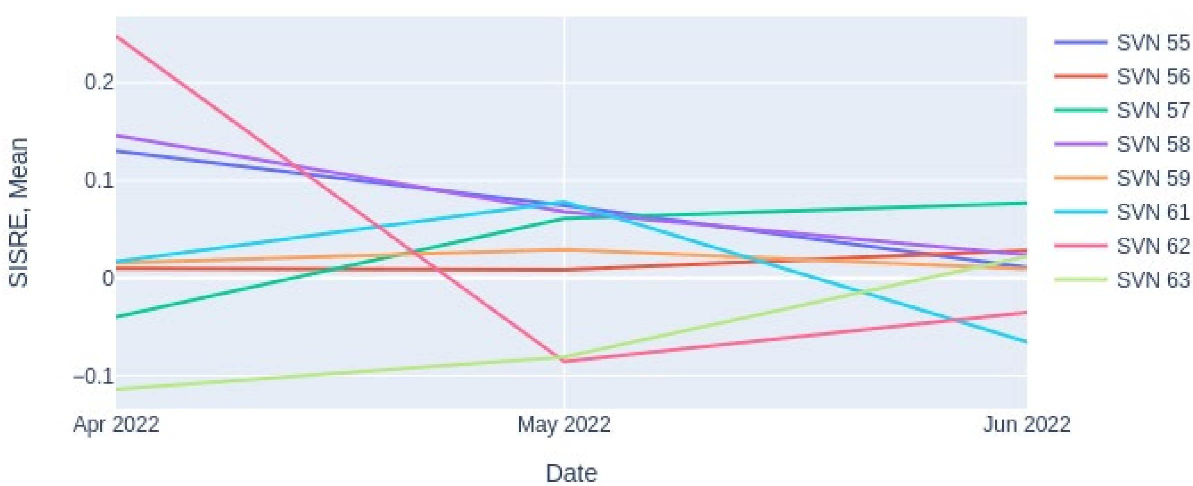


**Figure 2-16. Monthly Mean SISRE for SVN 55–SVN 63: 2nd Quarter 2022**

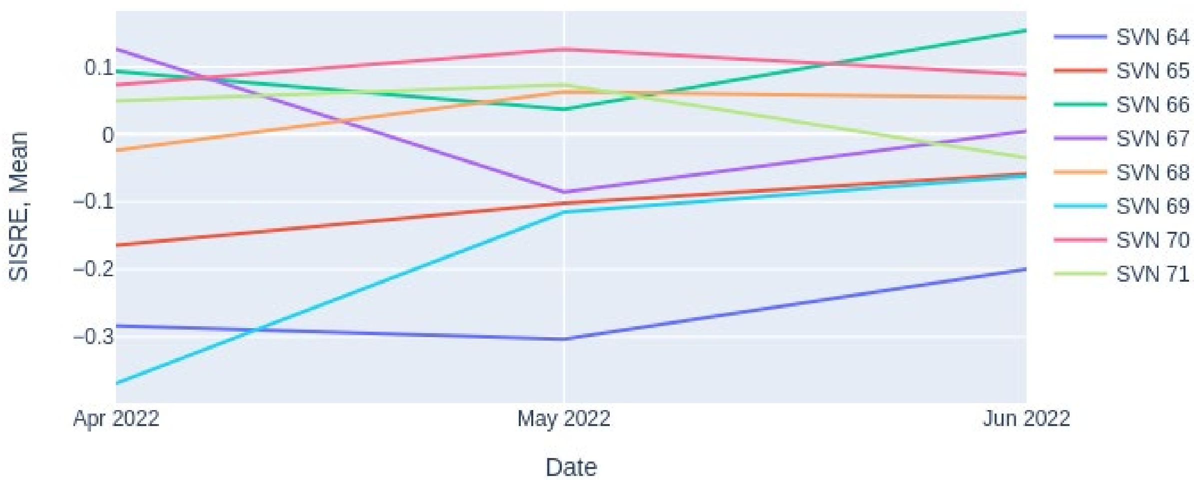


**Figure 2-17. Monthly Mean SISRE for SVN 64–SVN 71: 2nd Quarter 2022**

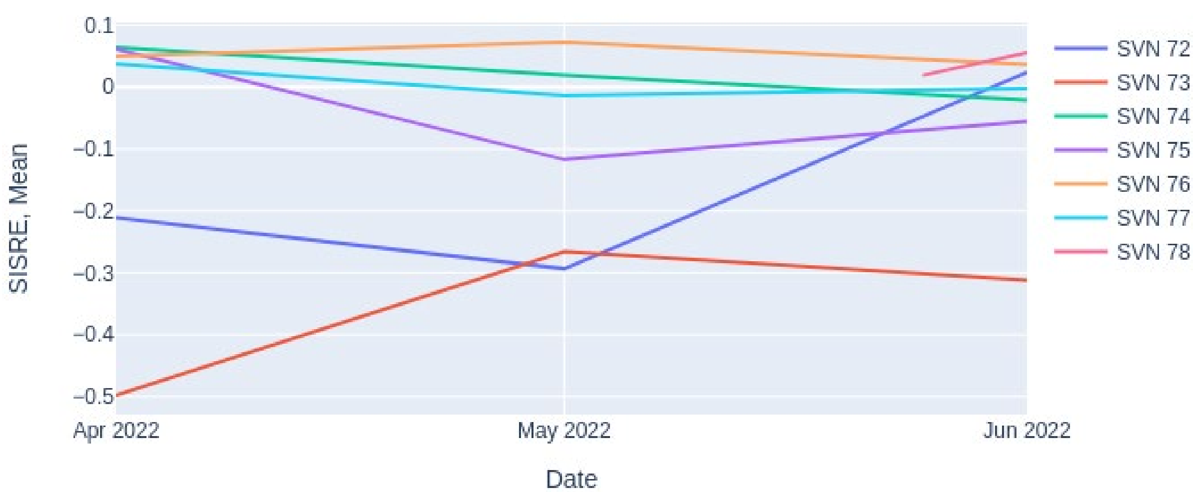


**Figure 2-18. Monthly Mean SISRE for SVN 72–SVN 78: 2nd Quarter 2022**

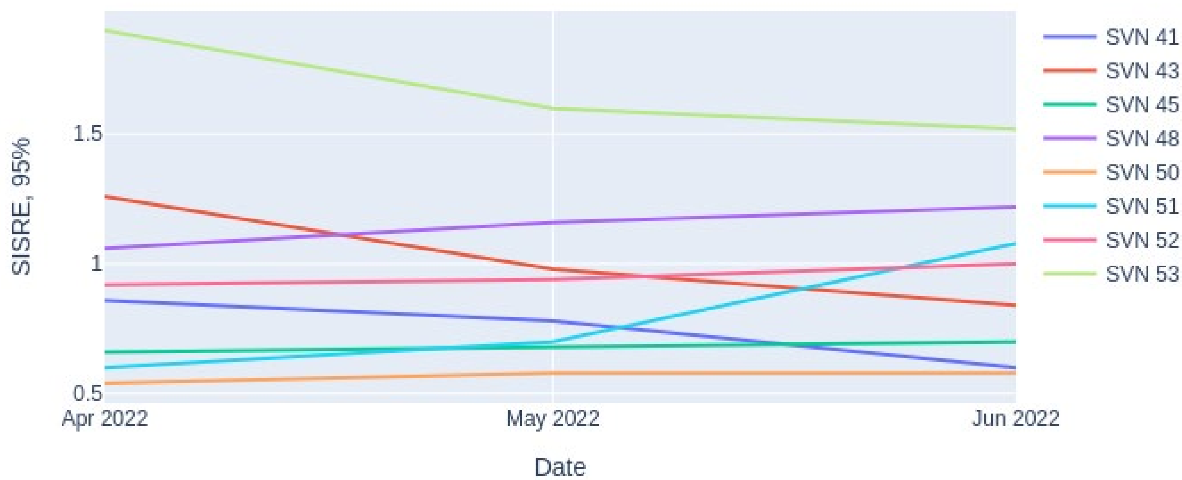


**Figure 2-19. Monthly 95% SISRE for SVN 41–SVN 53: 2nd Quarter 2022**

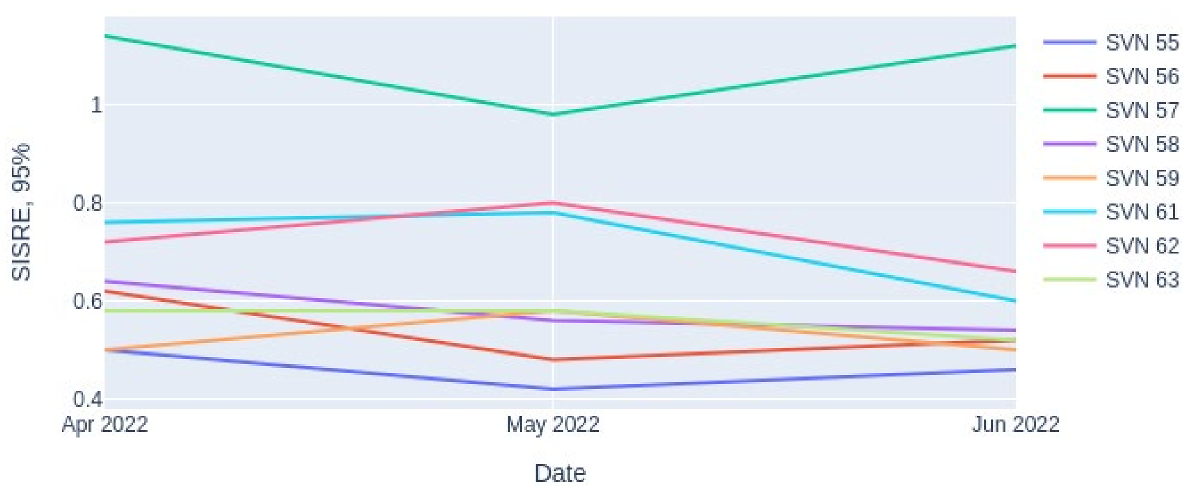


**Figure 2-20. Monthly 95% SISRE for SVN 55–SVN 63: 2nd Quarter 2022**

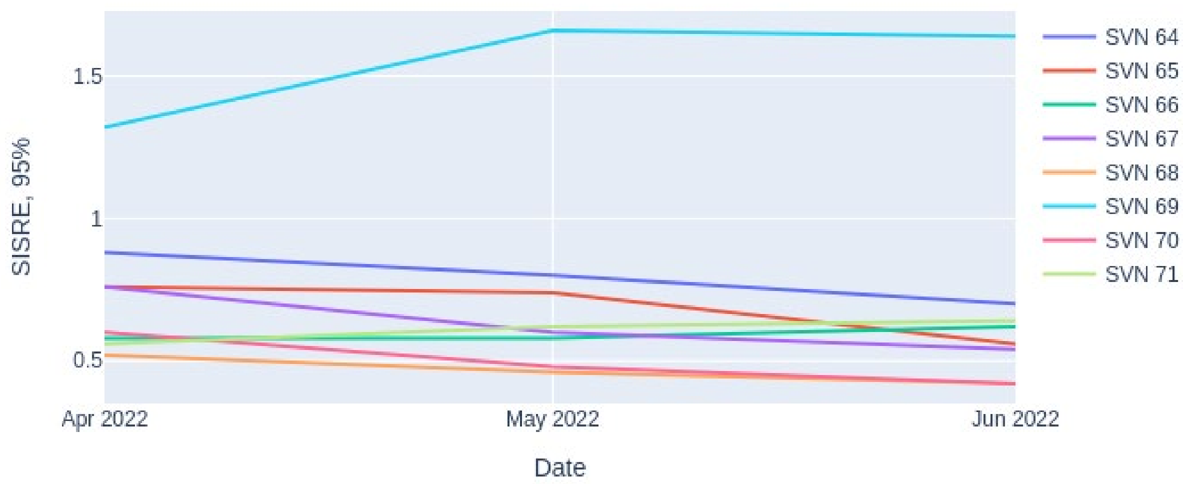


**Figure 2-21. Monthly 95% SISRE for SVN 64–SVN 71: 2nd Quarter 2022**

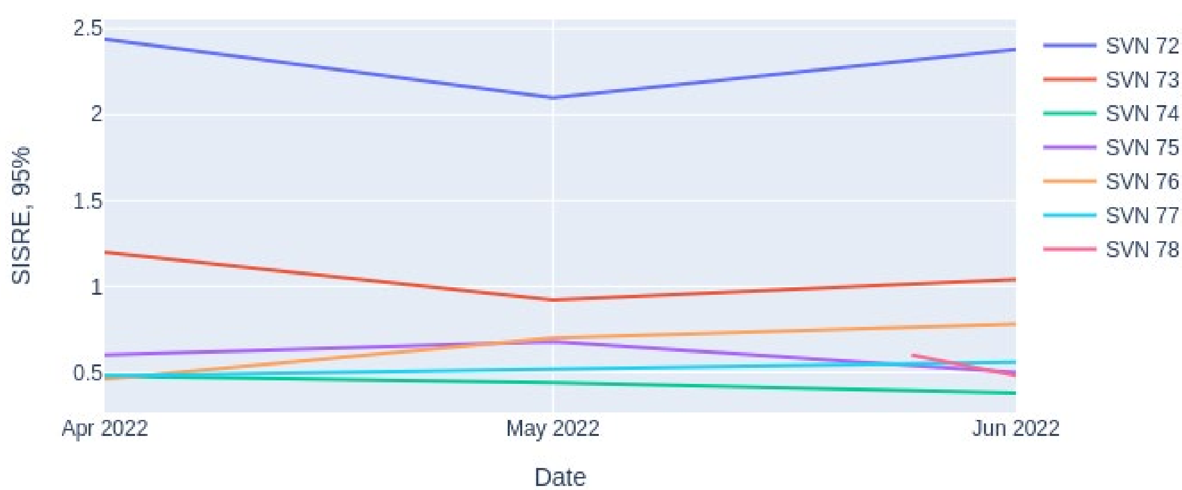


**Figure 2-22. Monthly 95% SISRE for SVN 72–SVN 78: 2nd Quarter 2022**

**Table 2-8. Monthly Mean and 95% SISRE: 2nd Quarter 2022**

| SVN | Mean (m) | | 95% (m) | |
|---|---|---|---|---|
| | Max | Min | Max | Min |
| 41 | 0.177 | 0.098 | 0.860 | 0.600 |
| 43 | 0.088 | 0.013 | 1.260 | 0.840 |
| 45 | 0.081 | 0.010 | 0.700 | 0.660 |
| 48 | 0.163 | 0.087 | 1.220 | 1.060 |
| 50 | 0.102 | 0.080 | 0.580 | 0.540 |
| 51 | 0.096 | 0.039 | 1.080 | 0.600 |
| 52 | 0.301 | 0.223 | 1.000 | 0.920 |
| 53 | 0.075 | 0.007 | 1.900 | 1.520 |
| 55 | 0.130 | 0.011 | 0.500 | 0.420 |
| 56 | 0.028 | 0.009 | 0.620 | 0.480 |
| 57 | 0.077 | 0.040 | 1.140 | 0.980 |
| 58 | 0.146 | 0.024 | 0.640 | 0.540 |
| 59 | 0.029 | 0.010 | 0.580 | 0.500 |
| 61 | 0.078 | 0.017 | 0.780 | 0.600 |
| 62 | 0.248 | 0.035 | 0.800 | 0.660 |
| 63 | 0.114 | 0.022 | 0.580 | 0.520 |
| 64 | 0.303 | 0.199 | 0.880 | 0.700 |
| 65 | 0.164 | 0.059 | 0.760 | 0.560 |
| 66 | 0.154 | 0.037 | 0.620 | 0.580 |
| 67 | 0.127 | 0.005 | 0.760 | 0.540 |
| 68 | 0.063 | 0.024 | 0.520 | 0.420 |
| 69 | 0.369 | 0.062 | 1.660 | 1.320 |
| 70 | 0.126 | 0.073 | 0.600 | 0.420 |
| 71 | 0.073 | 0.035 | 0.640 | 0.560 |
| 72 | 0.293 | 0.024 | 2.440 | 2.100 |
| 73 | 0.498 | 0.266 | 1.200 | 0.920 |
| 74 | 0.064 | 0.020 | 0.480 | 0.380 |
| 75 | 0.117 | 0.055 | 0.680 | 0.500 |
| 76 | 0.073 | 0.037 | 0.780 | 0.460 |
| 77 | 0.038 | 0.002 | 0.560 | 0.480 |
| 78 | 0.056 | 0.019 | 0.600 | 0.480 |

### 2.2.3 URA Bounding of Nominal Accuracy

Nominal range error distribution is examined to evaluate how well the URA described the observed error distribution and to ensure that the Gaussian assumption is valid. MPE and UPE error distributions are evaluated in this section.

The MPE can take on the value of zero if the three orbital errors and the clock error are all simultaneously zero. The MPE can also sometimes switch rapidly between positive and negative values as the corresponding projections change. As a result, the MPE distribution is bimodal with a notch at zero and is not expected to be Gaussian even if all the underlying distributions were Gaussian. However, the UPE distribution will be Gaussian, both at each individual user location and aggregated across all user locations, if the underlying errors are Gaussian. Although the MPE distribution is not expected to be Gaussian, it is well suited to describe the tail behavior. MPE and UPE PDF and CDF are used to assess the error distribution [9].

Figure 2-23 shows the PDF MPE normalized by the URA across the constellation. The notch at zero is expected, as described above. Figure 2-24 to Figure 2-27 show 1-CDF of the normalized MPE errors by satellite, and they are shown by block type in Figure 2-28. The thick red line shows the expected value corresponding to the normal distribution with zero-mean and unit variance. This line is only extended down to the $10^{-5}$ probability level, which is the specified satellite fault rate in the GPS SPS PS. Gaussian bounding below this line is not required.

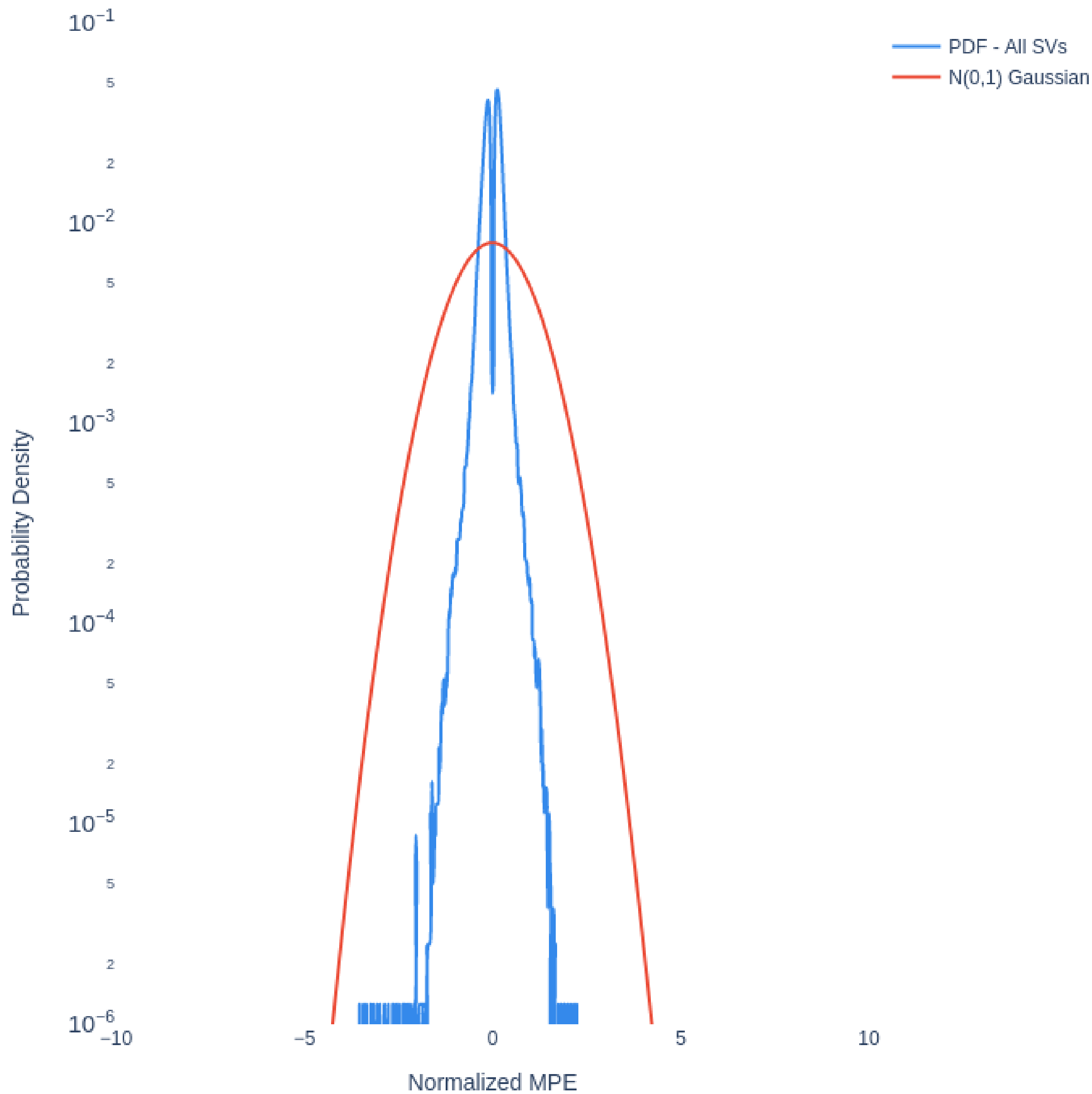


**Figure 2-23. PDF Normalized MPE Composite: 2nd Quarter 2022**

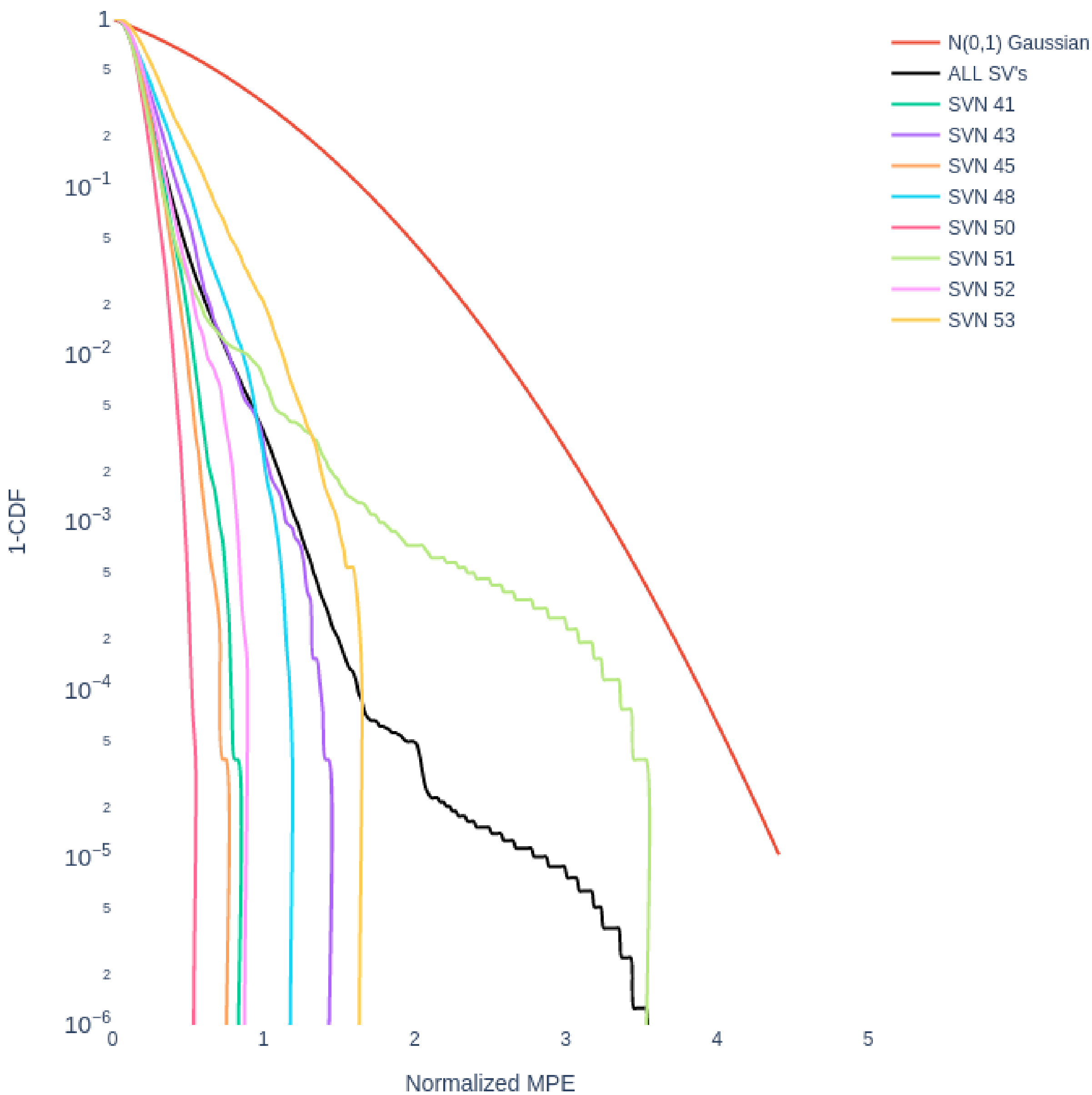


**Figure 2-24. 1-CDF Normalized MPE for SVN 41–SVN 53: 2nd Quarter 2022**

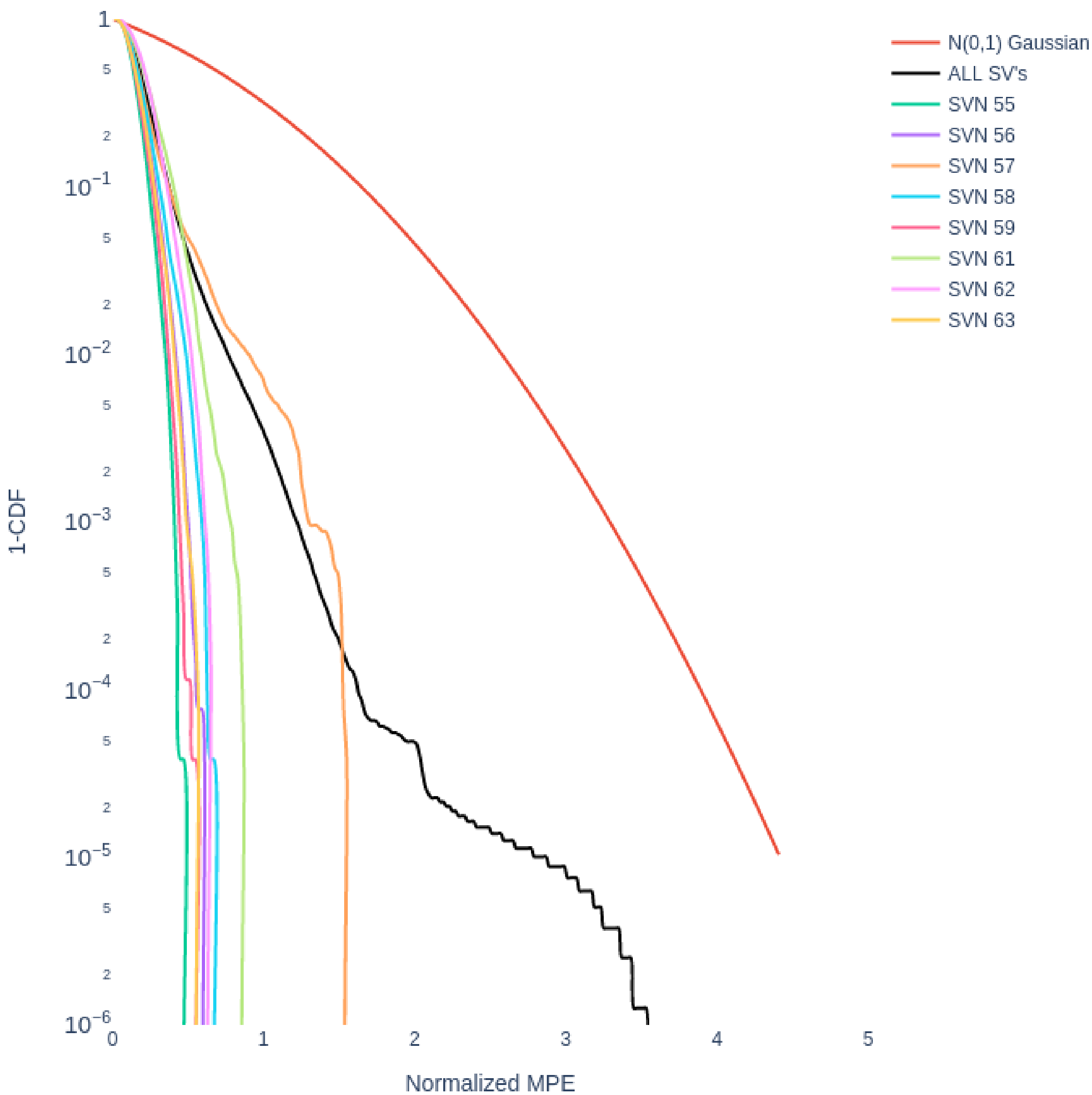


**Figure 2-25. 1-CDF Normalized MPE for SVN 55–SVN 63: 2nd Quarter 2022**

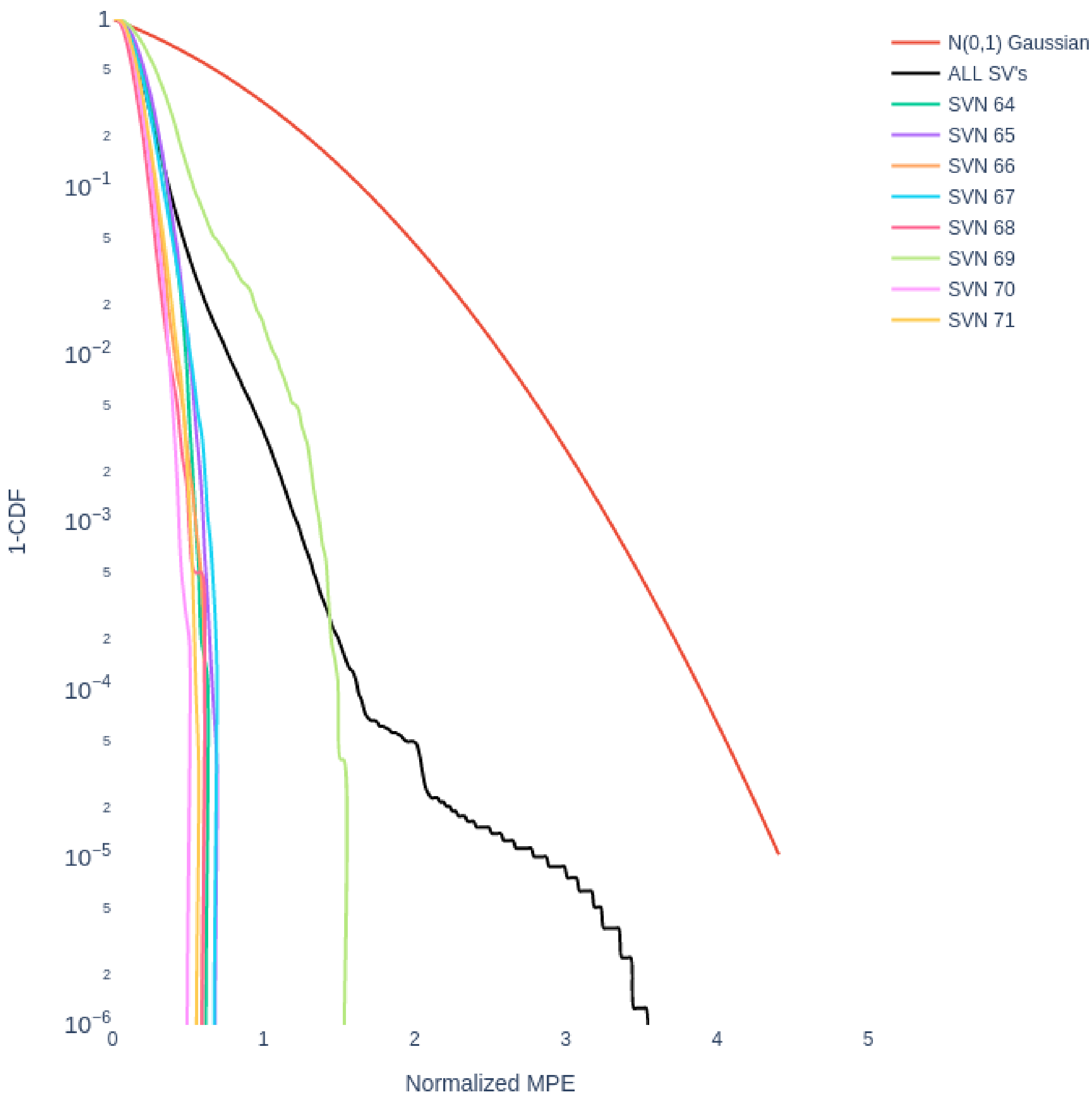


**Figure 2-26. 1-CDF Normalized MPE for SVN 64–SVN 71: 2nd Quarter 2022**

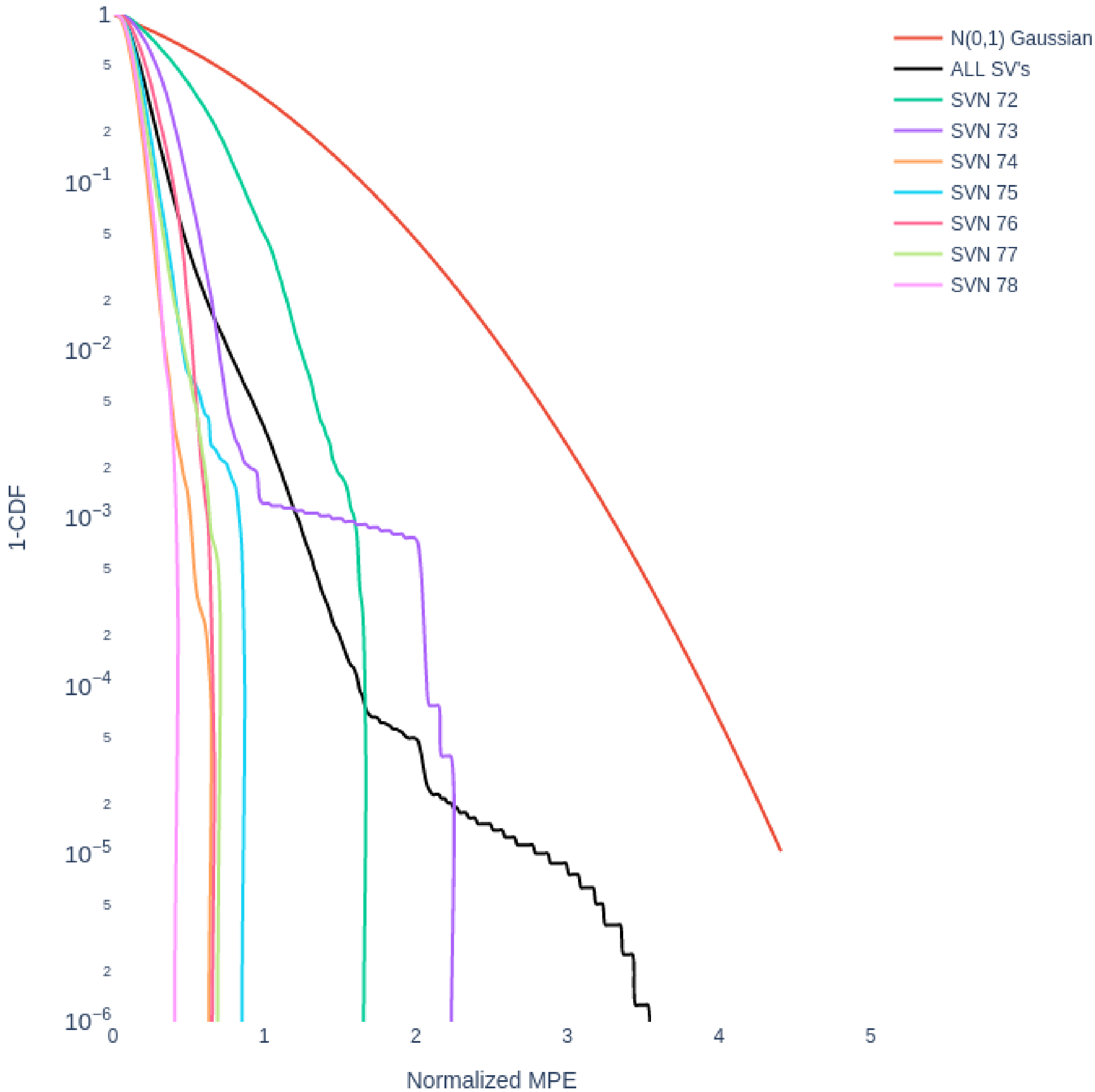


**Figure 2-27. 1-CDF Normalized MPE for SVN 72–SVN 78: 2nd Quarter 2022**

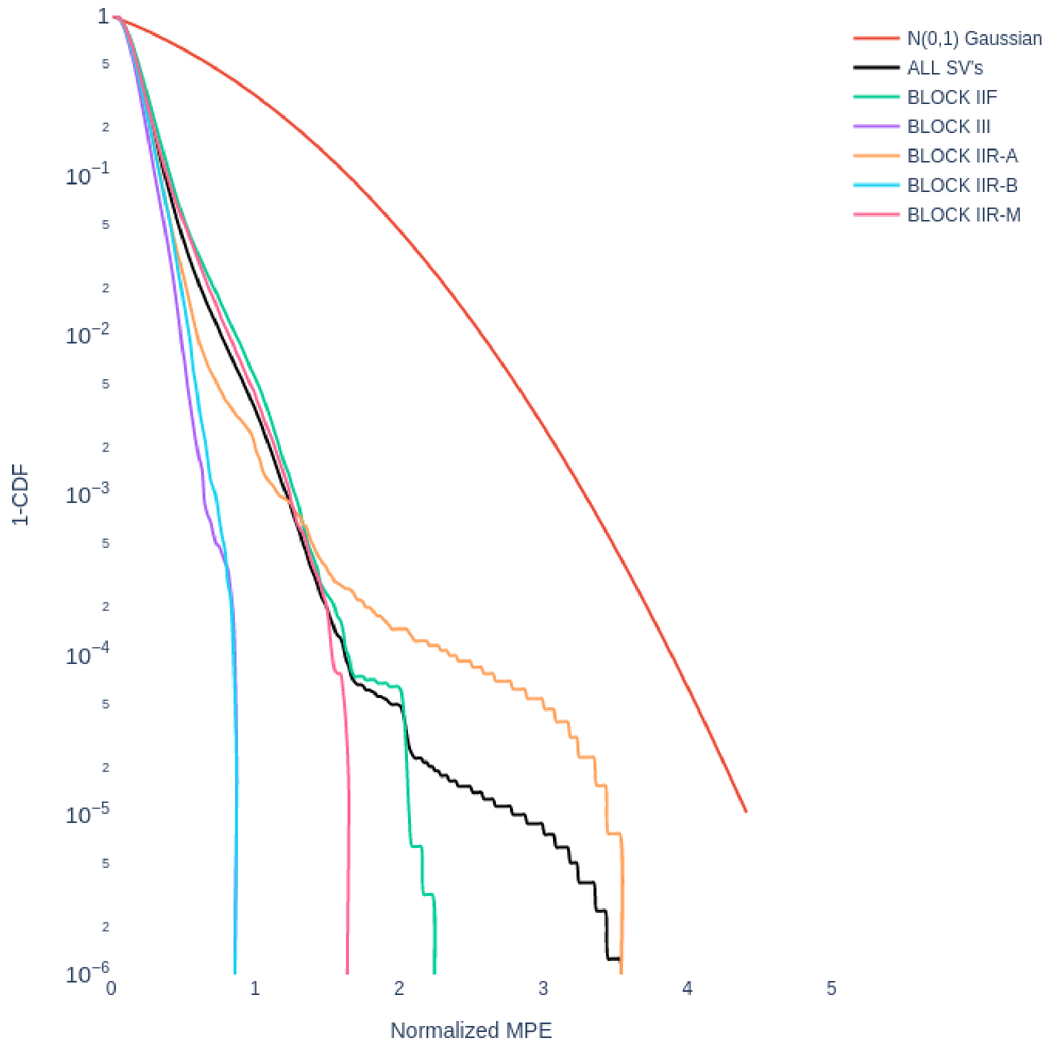


**Figure 2-28. 1-CDF Normalized MPE by Block Type: 2nd Quarter 2022**

Figure 2-29 shows the PDF of the composite normalized SISREs, which combines the instantaneous SISREs of all satellites at all 200 locations in the GPS constellation. Figure 2-30 to Figure 2-33 show the 1-CDF of the normalized SISRE errors combined across all 200 locations by satellite, and they are shown by block type in Figure 2-34. The thick red line represents the normal distribution with zero-mean and unity variance. This line is only extended down to the $10^{-5}$ probability level, which is the specified satellite fault rate in the GPS SPS PS. Gaussian bounding below this line is not required.

In this quarter, the nominal SISRE errors were described conservatively by the broadcast URA.

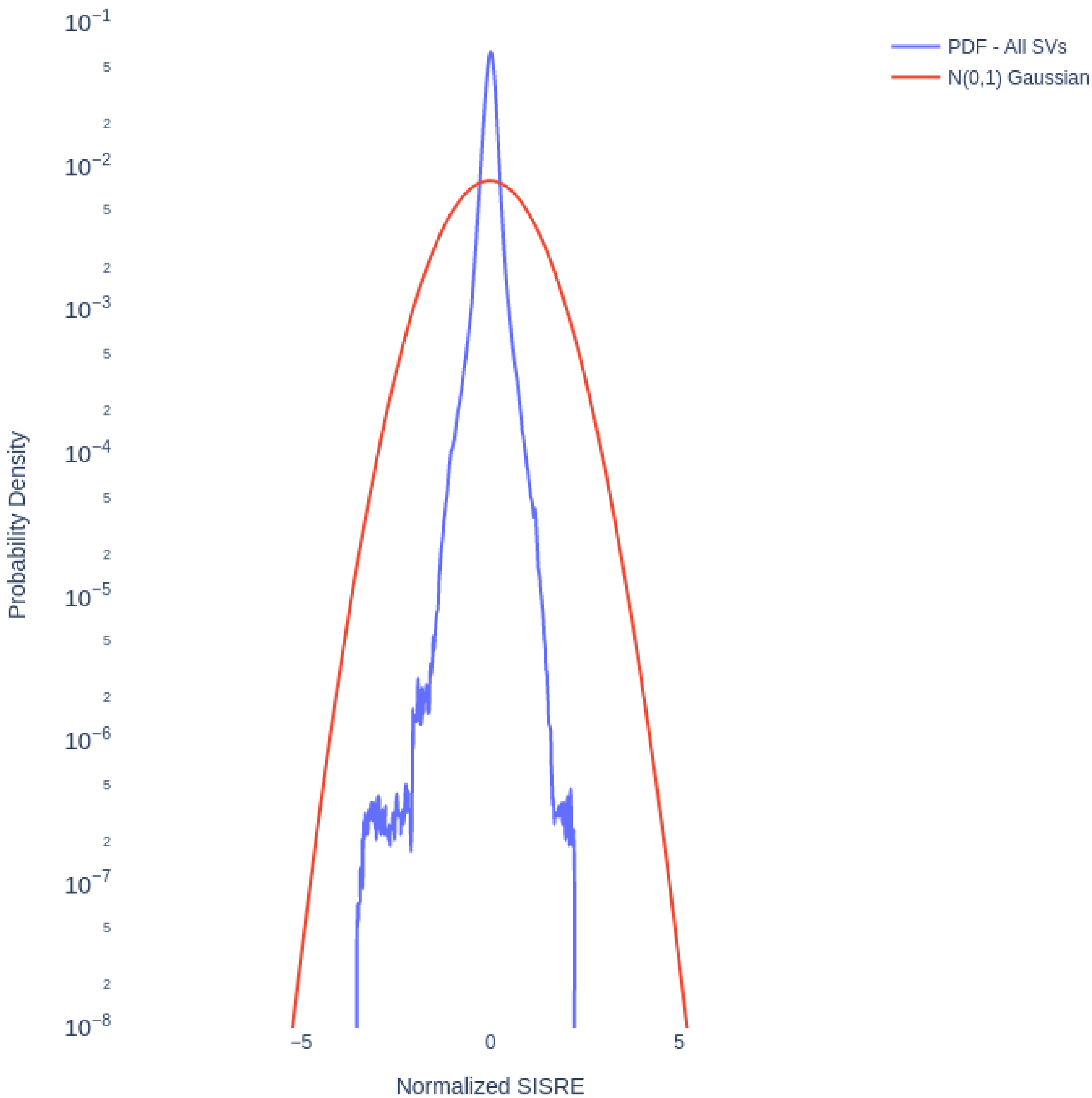


**Figure 2-29. PDF Normalized SISRE Composite: 2nd Quarter 2022**

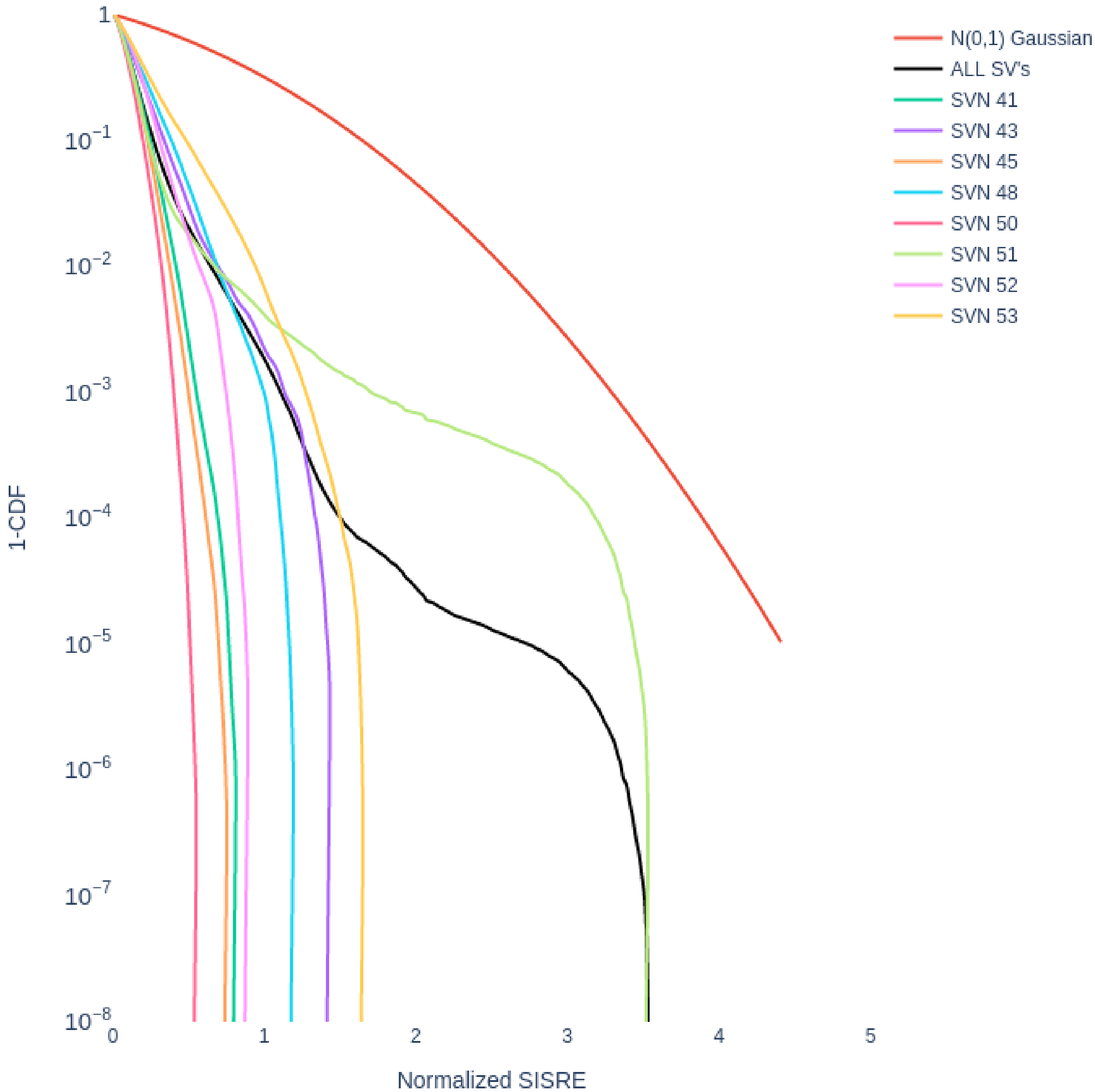


**Figure 2-30. 1-CDF Normalized SISRE for SVN 43–SVN 53: 2nd Quarter 2022**

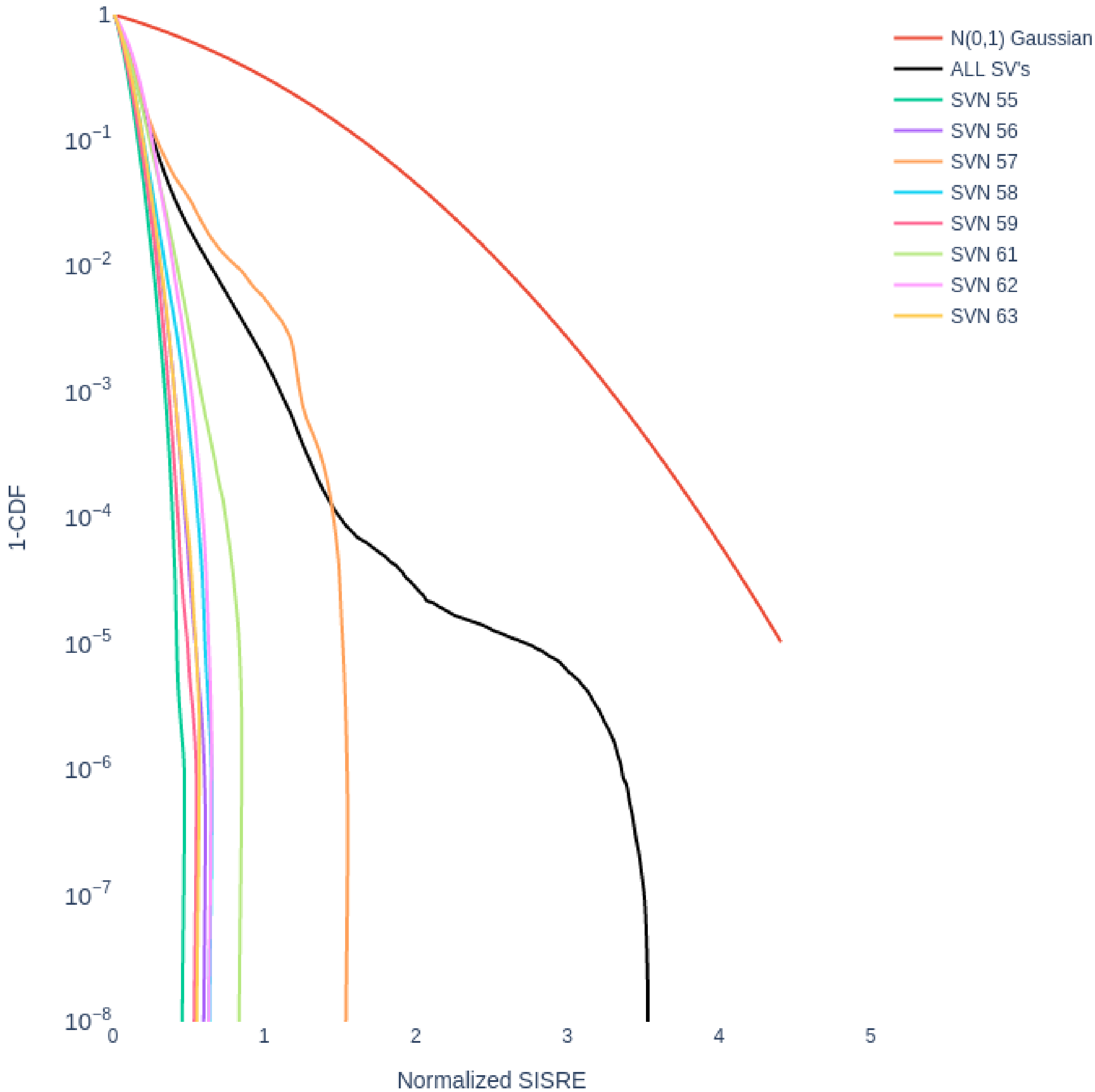


**Figure 2-31. 1-CDF Normalized SISRE for SVN 55–SVN 63: 2nd Quarter 2022**

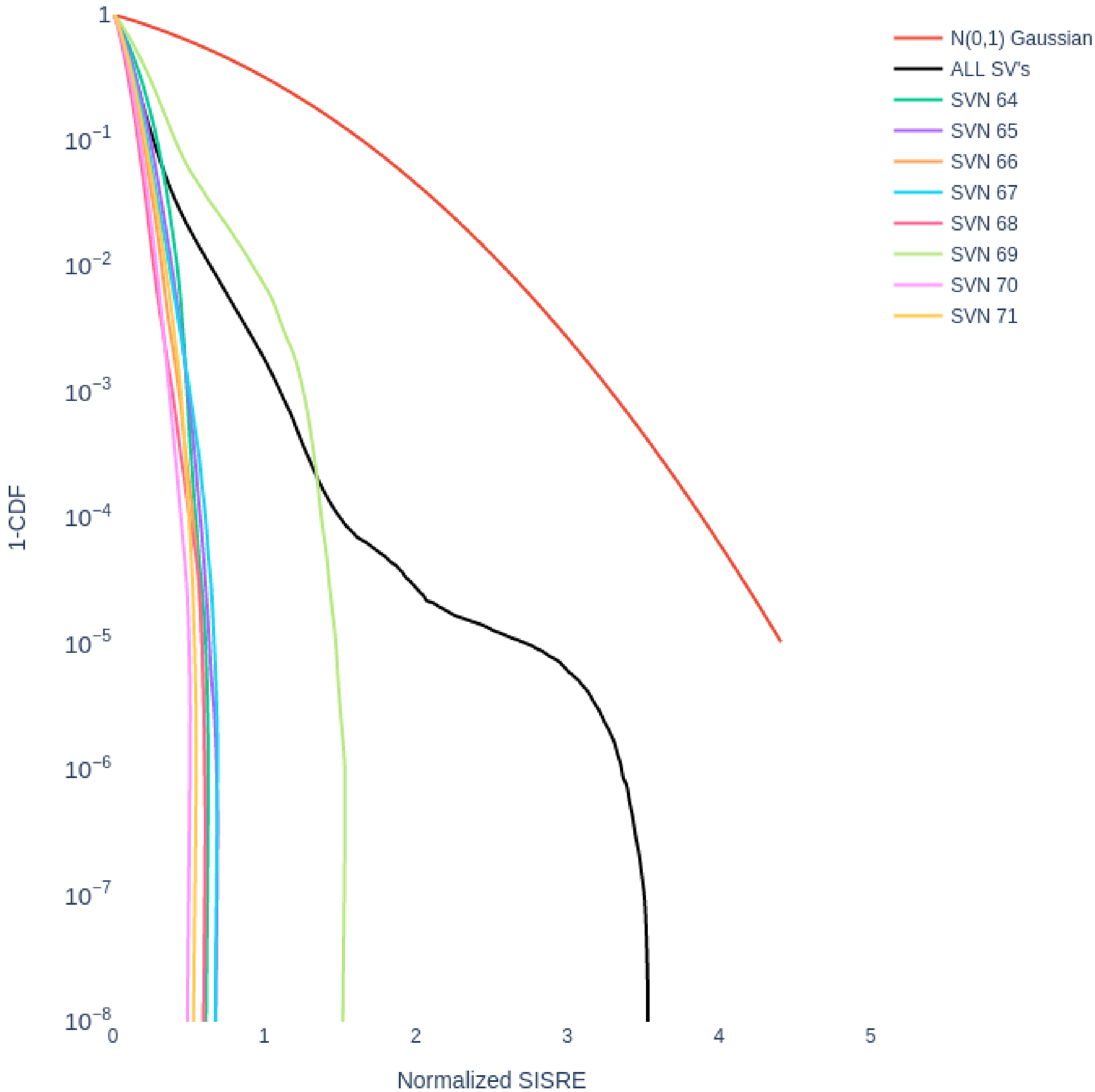


**Figure 2-32. 1-CDF Normalized SISRE for SVN 64–SVN 71: 2nd Quarter 2022**

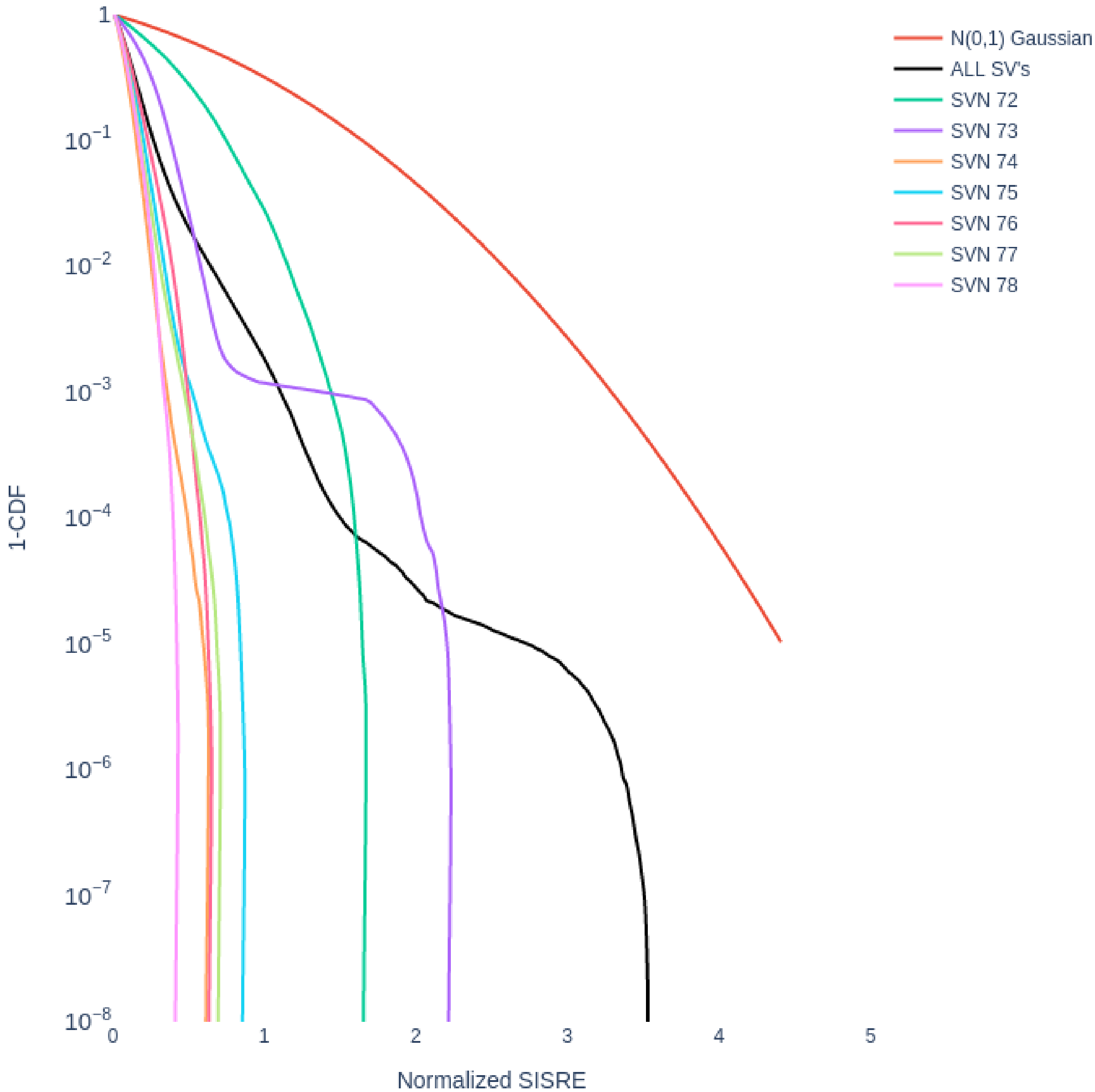


**Figure 2-33. 1-CDF Normalized SISRE for SVN 72–SVN 78: 2nd Quarter 2022**

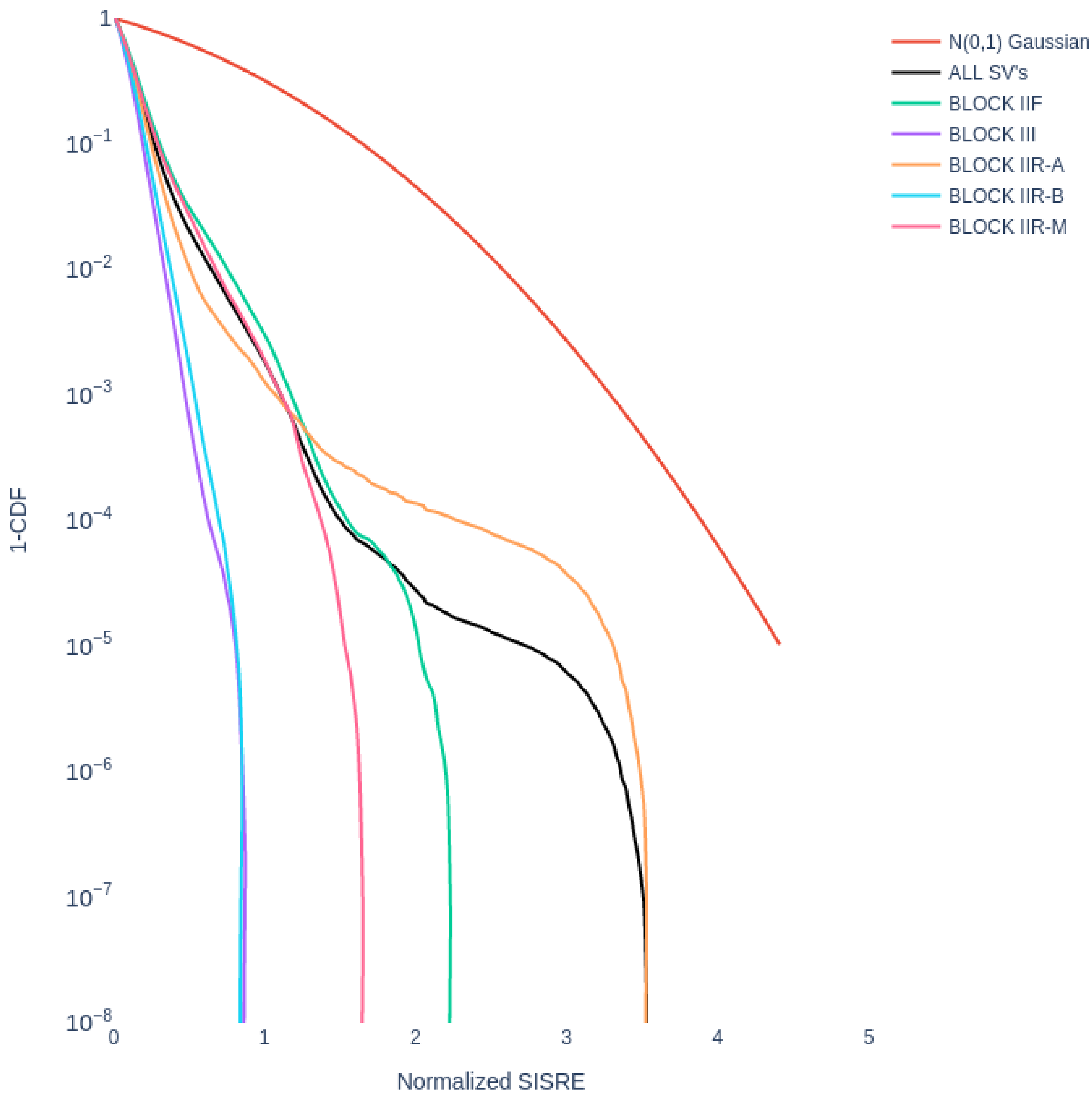


**Figure 2-34. 1-CDF Normalized SISRE by Block Type: 2nd Quarter 2022**

The overbounding sigma and the ratio of the overbound sigma to the broadcast URA are examined to evaluate how well the nominal errors are bounded by the broadcast URA and to what degree of margin. This evaluation attempts to separate the effect of quantization of the URA values from the ground system's ability to estimate the internal quantized value. Previous work has found that GPS increases the URA faster than the error actually increases; therefore, lumping all URA values together in the evaluation gave better results, which may be optimistic. More details on error bounding may be found in previous works [9, 13]. Since the URA value of 2.4 m is the most frequently broadcast value at 94.575% of the time this quarter, bounding is evaluated for errors when URA is 2.4 m and for the aggregated URA values. The ratio of less than 1 indicates the broadcast URA bounds the nominal error with a margin.

The ratio of the overbounding sigma to the broadcast URA is shown in Table 2-9. This ratio, or alpha value, is the smallest margin of the actual distribution to the Gaussian distribution. The overbounding sigma is formed by finding the minimum Gaussian value that bounds the SISRE CDF for each satellite at each error value. Alpha is the ratio between the points on the Gaussian curve and observed error curve with the smallest difference. Small regions of the curves are ignored during evaluation to account for convergence around the origin. The Y-axis data must be between 0.000095 and 0.5, and the X-axis data must be between 0.1 and 4.42. Figure 2-35 shows the ratio of the bounding sigma for URA at 2.4 m only. Table 2-9 shows the ratio of the bounding sigma to the broadcast URA of 2.4 m and for the combined broadcast URA values for each satellite.

For this quarter, the alpha values for the URA of 2.4 m only were very similar to the alpha values of the combined URAs. The largest alpha value was 0.822 on SVN 51. The bounding sigmas were below 1.973 m for the aggregate of each individual satellite, indicating a margin of URA bounding nominal errors.

**Table 2-9. Ratio of Bounding Sigma to URA: 2nd Quarter 2022**

| SVN | Ratio for URA=2.4m Only | Ratio for All URAs |
|---|---|---|
| 41 | 0.180 | 0.178 |
| 43 | 0.357 | 0.357 |
| 45 | 0.159 | 0.158 |
| 48 | 0.305 | 0.305 |
| 50 | 0.126 | 0.125 |
| 51 | 0.822 | 0.822 |
| 52 | 0.238 | 0.237 |
| 53 | 0.396 | 0.390 |
| 55 | 0.105 | 0.105 |
| 56 | 0.125 | 0.125 |
| 57 | 0.397 | 0.391 |
| 58 | 0.146 | 0.146 |
| 59 | 0.114 | 0.114 |
| 61 | 0.192 | 0.192 |
| 62 | 0.183 | 0.183 |
| 63 | 0.126 | 0.126 |
| 64 | 0.188 | 0.188 |
| 65 | 0.159 | 0.159 |
| 66 | 0.138 | 0.137 |
| 67 | 0.159 | 0.159 |
| 68 | 0.131 | 0.131 |
| 69 | 0.402 | 0.389 |
| 70 | 0.116 | 0.116 |
| 71 | 0.138 | 0.137 |
| 72 | 0.471 | 0.473 |
| 73 | 0.541 | 0.538 |
| 74 | 0.127 | 0.127 |
| 75 | 0.126 | 0.195 |
| 76 | 0.154 | 0.154 |
| 77 | 0.157 | 0.157 |
| 78 | 0.107 | 0.107 |

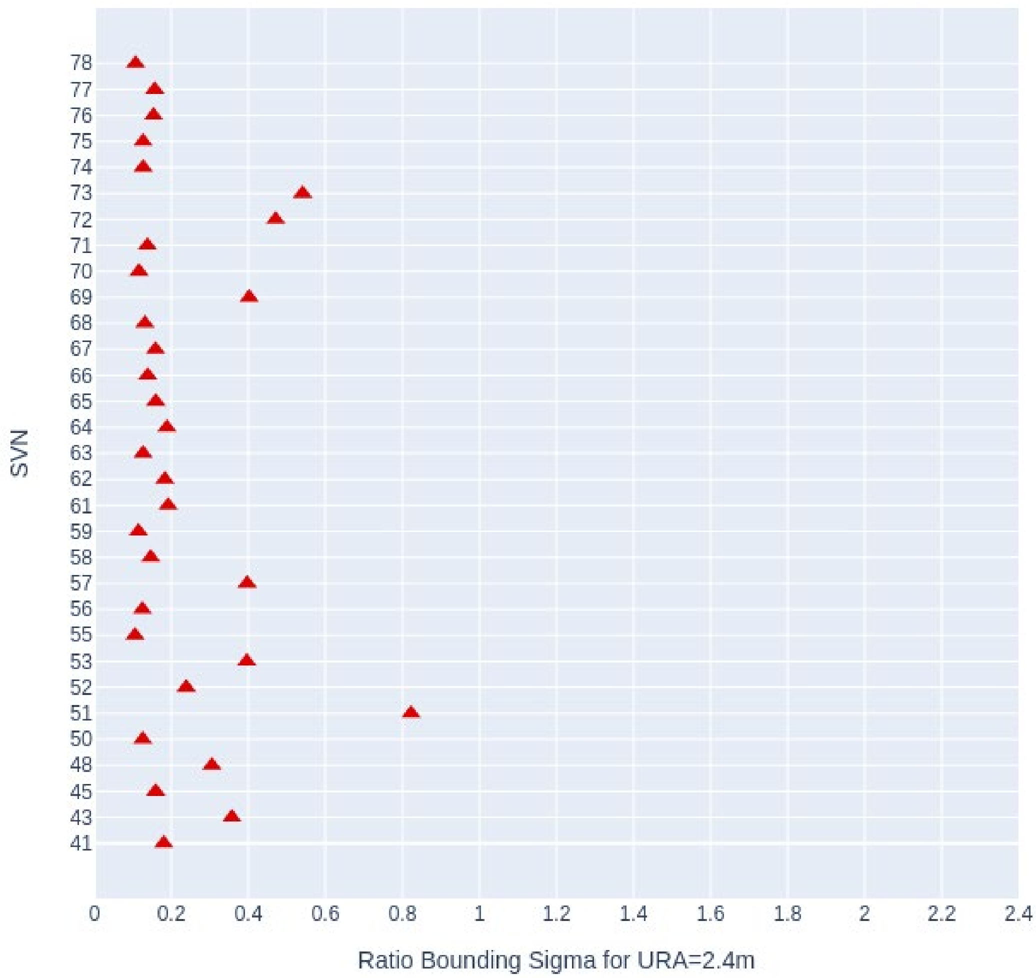


**Figure 2-35. Ratio of Bounding Sigma for URA=2.4 m: 2nd Quarter 2022**

### 2.2.4 URA Bounding of Nominal Position Accuracy

Nominal position errors are examined to ensure that individual satellite range errors, when combined, do not create position errors larger than the ones expected, assuming independent Gaussian range errors with a standard deviation given by the URA (the nominal error model), which is what the user assumes. It is important to assess the nominal position bounding for any possible user weights, because not all users will apply the same weights when combining the range errors. This can be achieved by examining the sum of the squares (SS) of the URA-normalized satellite range errors. (Satellite range errors exceeding 4.42* URA are excluded from this nominal assessment.)

The SS has two important properties. First, it is chi-square distributed assuming the nominal error model. Second, its square root is an upper bound of the ratio between the user error and the standard deviation as computed assuming the nominal error model [10, 11]. The observed SS distribution is expected to be well bounded by a chi-square distribution. If it is not, it means that the correlation in the measurements will cause the position errors to be larger than expected for some users. If the observed distribution is bounded by a unit Gaussian (for a range of probabilities), then the position errors are guaranteed to be bounded by a Gaussian with the expected standard deviation.

The SS is computed at each time epoch at the 200 user locations. It is obtained by subtracting a common-mode error from each SISRE (because this common error has no effect on the position error), normalizing each SISRE by the URA, and summing the squares of the resulting ratios.

Figure 2-36 shows the 1-CDF of the SS sample distribution (blue line), chi-square distribution (dotted red line), and zero mean unit Gaussian distribution (solid red line). The SS sample distribution is bounded by the chi-square distribution with ample margin. This indicates that the errors are consistent with an error model that is bounded by the nominal error model. In addition, the SS sample distribution is bounded by the Gaussian for all probabilities below 70%. This corresponds to the point in the CDFs in Figure 2-36 where the unit Gaussian (solid red curve) crosses the SS statistic (blue curve). Using the result outlined above, this means that those probabilities derived from the nominal error model are guaranteed to bound the distribution of the position error. This indicates that the unfaulted positioning errors are bounded by the nominal error model with significant margin.

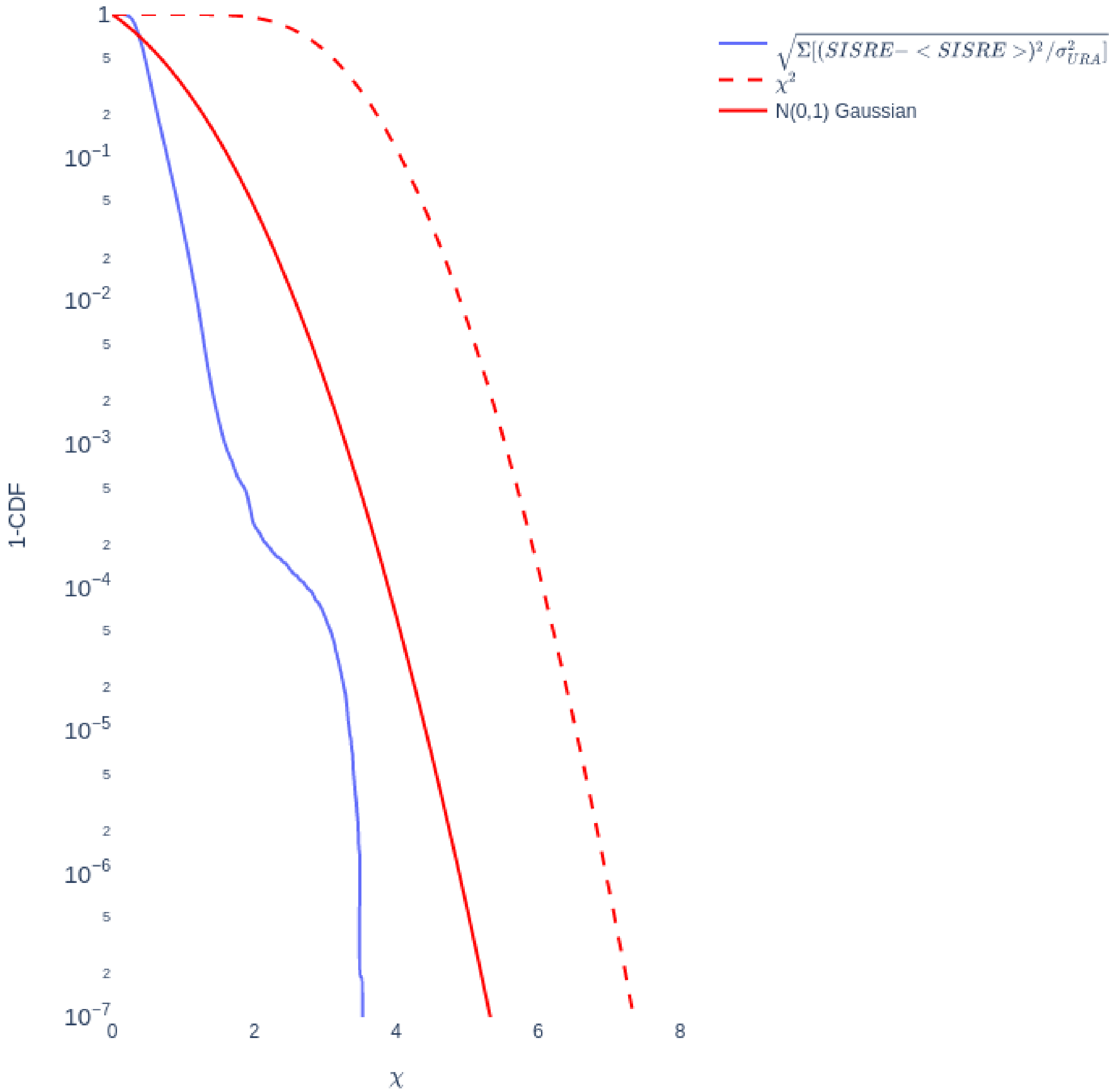


**Figure 2-36. 1-CDF Chi-Square of Normalized SISREs: 2nd Quarter 2022**

## 2.3 Fault Probability

At the time of this writing, no final decision was made on the format of the ISM message. In particular, fault rate information may be conveyed as an actual fault rate or as a probability of failure over a specified period of time. In this report, we present the fault rate only. The state fault probability can be obtained easily by multiplying the fault rate by the MFD. As the standardization process evolves, the approved approach or approaches will be presented in this section.

The critical fault parameters for ARAIM are the $R_{sat}$ and $P_{sat}$, the $R_{const}$ or $P_{const}$, and the MFD. These three parameters are based upon GPS CSP commitments and are supported by observational history. This section assesses the GPS constellation observed fault rates and MFD to ensure that they are consistent with CSP commitments (see Table 2-1). To do so requires the evaluation of GPS fault history, including satellite and constellation fault rates based on actual historical data.

Table 2-10 lists the known GPS constellation faults and durations since January 1, 2008. These faults have been discussed in a previous paper [10].

**Table 2-10. GPS Faults From January 1, 2008 to June 30, 2022 [10]**

| SVN | PRN | Date | Time of Fault (UTC) | Fault Duration | Description |
|---|---|---|---|---|---|
| 25 | 25 | 6/26/2009 | 09:05 – 09:45 | 40 minutes | A clock jumped 20 m at 09:05 causing the error to exceed 4.42*URA. URA was 2.4 m. Orbit was not affected, and the satellite was healthy. At 09:45, 155 of 156 IGS stations stopped tracking the satellite. Normal tracking of the satellite was resumed at 10:23 with a new ephemeris update that set the satellite to unhealthy. The lone receiver had only started tracking the satellite at 09:44:30 with discontinuities in pseudorange. |
| 38 | 8 | 11/5/2009 | 18:45 – 19:02 | 17 minutes | A clock ramp occurred at 18:15 causing the error to exceed 4.42*URA at 18:44:45. URA was 2.4 m. Orbit was not affected and the satellite was healthy. All 135 IGS stations stopped tracking the satellite at 19:02. At approximately 19:28, regular transmission resumed with a new ephemeris update that set the satellite to unhealthy. |

| SVN | PRN | Date | Time of Fault (UTC) | Fault Duration | Description |
|---|---|---|---|---|---|
| 30 | 30 | 02/22/2010 | 20:45 – 20:52 | 7 minutes | A clock ramp occurred at 20:30 causing the error to exceed 4.42*URA at 20:45. URA was 2.4 m. Orbit was not affected and the satellite was healthy. All 108 IGS stations stopped tracking the satellite at 20:52. At approximately 2:15, regular transmission resumed with a new ephemeris update that set the satellite to unhealthy. |
| 39 | 9 | 04/25/2010 | 19:40 – 19:55 | 15 minutes | At 19:26, a new ephemeris update introduced a 40 m cross-track error with the URA=2.4 m. The MPE error barely exceeded the 4.42*URA at 19:40. The fault was corrected at 19:55 with a new ephemeris update. The satellite health was set to healthy the entire time. |
| 59 | 19 | 06/17/2012 | 00:10 – 00:36 | 26 minutes | At 00:10, a new ephemeris update introduced a 1700 m cross-track error with the URA=2.4 m. The MPE error exceeded the 4.42*URA. The fault was corrected at 00:37 with a new ephemeris update. The satellite health was set to healthy the entire time. |

Each of the 5 known faults lasted less than 1 hour and the average across all 5 faults was 21 minutes. Therefore, the committed value of MFD of 1 hour appears to be valid and conservative.

Independent, single satellite faults are referred to as narrow faults, and simultaneous or overlapping satellite faults that originate from a common cause within a single constellation, are referred to as wide faults. The narrow fault rate computation uses a 30-satellite constellation and takes into account the historical satellite faults listed in Table 2-10. Figure 2-37 shows the times of historical single-fault events and their effect on the fault rate. The rates are shown for different time windows computed at 6-month increments, with no satellite fault since 2012. The fault rate determination has been discussed in previous work [12], and the method recommended in the previous work suggested taking the maximum value of the sliding 48-month average, which corresponds to a number well below $10^{-5}$.

In this quarter, no satellite or constellation fault events were observed.

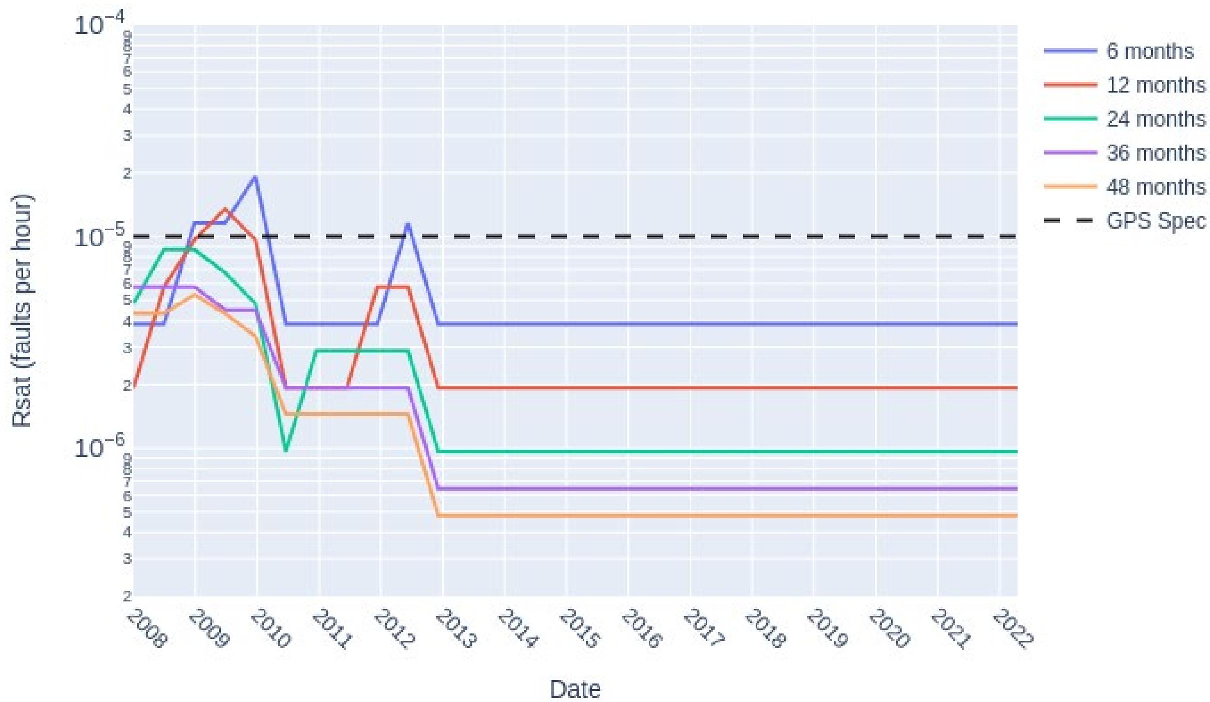


**Figure 2-37. Estimated Satellite Narrow Fault Rate**

### 2.3.1 List of Events

Table 2-11 lists all events for this quarter. Events include potential SIS anomalies and any other issues that occurred during this reporting period. Analyses of events that merit more detailed investigations are documented in the individual ARAIM PAN reports, which may be found at https://www.nstb.tc.faa.gov/araim-archive.html and by hyperlink in Table 2-11.

**Table 2-11. Events**

| SVN | PRN | Start | End | Description |
|---|---|---|---|---|
| 45 | 21 | 08-Apr-22 03:15 UTC | 08-Apr-22 13:42 UTC | SVN45 (PRN21) was set unusable. See NANU2022019. |
| 53 | 17 | 21-Apr-22 16:13 UTC | 21-Apr-22 16:13 UTC | SVN53 (PRN17) was set unusable. See NANU2022021. |
| 75 | 18 | 19-May-22 20:19 UTC | 19-May-22 20:19 UTC | SVN75 (PRN18) was set unusable. See NANU2022023. |
| 78 | 11 | 25-May-22 17:12 UTC | N/A | SVN78 (PRN11) was set usable. See NANU2022025. |
| 58 | 12 | 26-May-22 17:26 UTC | 27-May-22 00:07 UTC | SVN58 (PRN12) was set unusable. See NANU2022026. |
| 55 | 15 | 07-Jun-22 13:17 UTC | 07-Jun-22 20:44 UTC | SVN55 (PRN15) was set unusable. See NANU2022028. |
| 68 | 9 | 24-Jun-22 08:15 UTC | 24-Jun-22 13:35 UTC | SVN68 (PRN09) was set unusable. See NANU2022030. |
| 72 | 8 | 30-Jun-22 07:36 UTC | 30-Jun-22 14:31 UTC | SVN72 (PRN08) was set unusable. See NANU2022032. |

# 3. REFERENCES


1. ARAIM Concept of Operation, Working Group C Service Evolution Subgroup, April 23, 2018.

2. Department of Defense, "Global Positioning System Standard Position Service Performance Standard," 5th Edition, April 2020.

3. National Geospatial-Intelligence Agency, NGA/GPS 5 Minute Ephemeris SP3 Format Description, https://earth-info.nga.mil/index.php?dir=gnss&action=gnss, last accessed June 28, 2022.

4. International GNSS Service (IGS), "RINEX The Receiver Independent Exchange Format," Version 3.03, August 2, 2020, https://kb.igs.org/hc/en-us/articles/201096516-IGS-Formats

5. National Aeronautics and Space Administration, CDDIS, https://cddis.nasa.gov/, last accessed June 2, 2020.

6. Scripps Orbit and Permanent Array Center/California Spatial Reference Center, http://sopac-csrc.ucsd.edu/, last accessed June 2, 2020.

7. National Geospatial-Intelligence Agency, GPS and Earth Orientation Products, https://earth-info.nga.mil/GandG/update/index.php?action=home#tab_gnss, last accessed November 9, 2020.

8. Heng, L., "Safe Satellite Navigation with Multiple Constellations: Global Monitoring of GPS and GLONASS Signal-in-Space Anomalies," 2012.

9. Walter, T., Gunning, K., Phelts, E., and Blanch, J., "Validation of Unfaulted Error Bounds for ARAIM," NAVIGATION Journal of The Institute of Navigation, February 2018.

10. Walter, T. and Blanch, J., "Characterization of GNSS Clock and Ephemeris Errors to Support ARAIM," Proceedings of the ION 2015 Pacific PNT Meeting, Honolulu, Hawaii, April 2015.

11. Walter, T., Blanch, J., Enge, P., "Evaluation of Signal in Space Error Bounds to Support Aviation Integrity," NAVIGATION, Journal of The Institute of Navigation, Vol. 57, No. 2, Summer 2010, pp. 101-113.

12. Walter, T., Blanch, J., Joerger, M., and Pervan, B., "Determination of Fault Probabilities for ARAIM," Proceedings of IEEE/ION PLANS 2016, Savannah, Georgia, April 2016.

13. Blanch, J., Walter, T., and Enge, P., "Gaussian Bounds of Sample Distributions for Integrity Analysis," in IEEE Transactions on Aerospace and Electronic Systems, Vol. 55, No. 4, pp. 1806-1815, Aug. 2019, doi: 10.1109/TAES.2018.2876583.

## APPENDIX A: GLOSSARY AND ACRONYMS

| | |
|---|---|
| ARAIM | Advanced Receiver Autonomous Integrity Monitoring |
| $b_{nom0}$ | URA-independent overbound of nominal range bias error |
| CDDIS | Crustal Dynamics Data Information System (IGS archive site) |
| CDF | Cumulative Distribution Function |
| cm | Centimeter |
| CSP | Constellation Service Provider |
| ECEF | Earth-Centered, Earth-Fixed |
| FAA | Federal Aviation Administration |
| GNSS | Global Navigation Satellite Systems |
| GPS | Global Positioning System |
| IAURA | Integrity Assured User Range Accuracy. The IAURA is a conservative representation of the upper bound on each satellite's expected RMS URE performance over the curve fit interval represented by the NAV data from which the URA is read. |
| IGS | International GNSS Service |
| ISM | Integrity Support Message |
| LNAV | Legacy Navigation Message |
| m | Meter |
| MFD | Mean Fault Duration |
| MPE | Maximum Projected Error |
| MSI | Misleading Signal-in-Space Information |
| NANU | Notice Advisory to Navstar Users |
| NGA | National Geospatial-Intelligence Agency |
| NTE | Not to Exceed (i.e., tolerance limit) |
| PAN | Performance Analysis Report |

| | |
|---|---|
| $P_{const}$ | Probability of multiple satellites being in a common-cause MSI faulted state at a given time. |
| PDF | Probability Density Function |
| PRN | Pseudo-Random Noise |
| PS | Performance Standard |
| $P_{sat}$ | Probability of a satellite being in an MSI faulted state at a given time |
| RAC | Radial-along track-cross track. Orbital coordinate system. |
| RINEX | Receiver Independent Exchange |
| $R_{sat}$ | Rate of a single satellite fault |
| SF | Single-Frequency |
| SIS | Signal-in-Space |
| SISRE | Signal-in-Space Range Error |
| SOPAC | Scripps Orbit and Permanent Array Center (IGS archive site) |
| SP3 | Standard Product #3 |
| SPS | Standard Positioning Service. The GPS broadcast signals, as defined in IS-GPS-200 and IS-GPS-705, providing constellation performance to peaceful civil, commercial, and scientific users, as established in the SPS Performance Standard (SPS PS), in accordance with U.S. Government policy. |
| SS | Sum of the Squares |
| SV | Space vehicle |
| SVN | Space vehicle number |
| $t_{CORREL}$ | Correlation time constant |
| UMSI | Unalerted Misleading Signal Information. |
| UPE | User Projected Error |
| URA | User Range Accuracy. The URA is a conservative representation of each satellite's expected RMS URE performance over the curve fit interval represented by the NAV data from which the URA is read. |
| URE | User Range Error |

| | |
|---|---|
| U.S. | United States |
| UTC | Coordinated Universal Time |
| WAAS | Wide Area Augmentation System |
| $\gamma_{nom}$ | URA-dependent overbound of nominal range bias errors |